Preliminary stratigraphy and geochronology of the Hazelton Group, Kitsault River area, Stikine terrane, northwest British Columbia

Rebecca C. Hunter[1, a], and Bram I. van Straaten[1]

[1] British Columbia Geological Survey, Ministry of Energy, Mines and Petroleum Resources, Victoria, BC, V8W 9N3
[a] corresponding author: Rebecca.Hunter@gov.bc.ca

Recommended citation: Hunter, R.C., and van Straaten, B.I., 2020. Preliminary stratigraphy and geochronology of the Hazelton Group, Kitsault River area, Stikine terrane, northwest British Columbia. In: Geological Fieldwork 2019, British Columbia Ministry of Energy, Mines and Petroleum Resources, British Columbia Geological Survey Paper 2020-01, pp. 101-118.

Abstract

The Kitsault River area, at the southern end of the Iskut-Stewart mineral belt of northwestern Stikinia, hosts porphyry Cu-Au, porphyry-related gold, and precious metal-rich VMS deposits in Hazelton Group volcano-sedimentary rocks. Based on new mapping northwest and east of Kinskuch Lake, we further resolve stratigraphic relationships in the lower part of the Hazelton Group and recognize three new facies and two new sub-facies. Facies 1 and 3 consist of lapilli tuff to tuff breccia with hornblende-plagioclase-phyric clasts and minor interbedded epiclastic rocks. Facies 2 consists of predominantly epiclastic rocks. Facies 3 is further subdivided into sub-facies 3a, a distinctive unit of K-feldspar- and plagioclase-phyric flows and lapilli tuffs to tuff breccia and sub-facies 3b, a mixed volcano-sedimentary unit with local features indicating subaerial deposition. New U-Pb zircon data provide age constraints to the Hazelton Group in the area, including a maximum depositional age from detrital zircons (U-Pb, LA-ICPMS) of ca. 206 Ma (Rhaetian) for the onset of Hazelton Group volcanism. A monzonite dike from near the Homestake Ridge deposit gave an age of ca. 191 Ma (U-Pb CA-TIMS), indicating that Cu-Au mineralizing systems in the Kitsault River area are Early Jurassic. A felsic lapilli tuff from directly beneath the Wolf deposit yielded a crystallization age of ca. 178 Ma (U-Pb, LA-ICPMS), suggesting that upper parts of the Hazelton Group are developed in the Kitsault River valley area and host some VMS related mineralization. Consistent with this conclusion, a volcanic-derived sandstone sample from the southern shore of Kitsault Lake returned a detrital zircon maximum depositional age of ca. 169 Ma (U-Pb, LA-ICPMS). These upper Hazelton Group units differ from those in the Eskay rift and at the Anyox deposit, which contain abundant bimodal felsic and mafic volcanic rocks. Nonetheless, these coeval syngenetic mineralizing systems are likely related and we interpret that VMS mineralization in the Kitsault River area reflects hydro-magmatic fluids flowing along syndepositional faults to near-surface levels. Extensional processes that operated at Eskay may have extended into in the Kitsault River area but without producing a large rift basin.

Keywords: Kitsault River, Hazelton Group, Stikine terrane, Jurassic, VMS, Eskay rift, silver, copper, gold

1. Introduction

Northwest British Columbia is endowed with significant porphyry Cu-Au, epithermal Au, and volcanogenic massive sulphide (VMS) precious and base metal deposits in Triassic and Jurassic rocks of the Stikine terrane (also known as Stikinia), particularly volcano-sedimentary successions of the Hazelton Group and allied plutons (Fig. 1; Höy, 1991; Childe, 1997; Nelson et al., 2013; Logan and Mihalynuk, 2014; Barresi et al., 2015; Nelson et al., 2018). Richly endowed porphyry systems extend along the length of the Canadian Cordillera generated by Late Triassic to Early Jurassic arc magmatism (Nelson et al., 2013; Logan and Mihalynuk, 2014). Examples of deposits in the Stikine terrane include Big Missouri, Schaft Creek, Galore Creek/Copper Canyon, Red Chris, the KSM porphyry trend, and Red Mountain (Fig. 2). Similarly, epithermal precious metal hydrothermal systems formed in response to Early Jurassic volcanism and related plutonic activity (Diakow et al., 1991; Nelson et al., 2013; Logan and Mihalynuk, 2014) led to mineralization at the Toodoggone, Premier, Snip, and Bronson deposits (Fig. 2). During the Middle Jurassic, mineralizing systems evolved into VMS-type settings that were active during deposition of the upper part of the Hazelton Group (Gagnon et al., 2012). Primary examples include the Eskay Creek deposit (Au-rich; Barrett and Sherlock, 1996; Childe, 1996; MacDonald et al., 1996a; Roth et al., 1999; Sherlock et al., 1999; Barresi and Dostal, 2005) and the Anyox deposit (Fig. 2; Cu-rich; Smith, 1993; MacDonald et al., 1996b; Evenchick and McNicoll, 2002). All of these are hosted by the Iskut River Formation, a bimodal felsic-mafic volcanic and sedimentary rock succession that constitutes the fill of the Eskay rift (Gagnon et al., 2012; Nelson et al., 2013, 2018).

Detailed mapping of the Hazelton Group and better age constraints are vital for understanding the depositional and volcanic environments that were responsible for VMS and epithermal-type mineralizing systems throughout western Stikinia. Herein we report the preliminary results of detailed mapping and geochronology in the Kitsault River area (Figs. 2, 3). We: 1) present composite stratigraphic sections based on

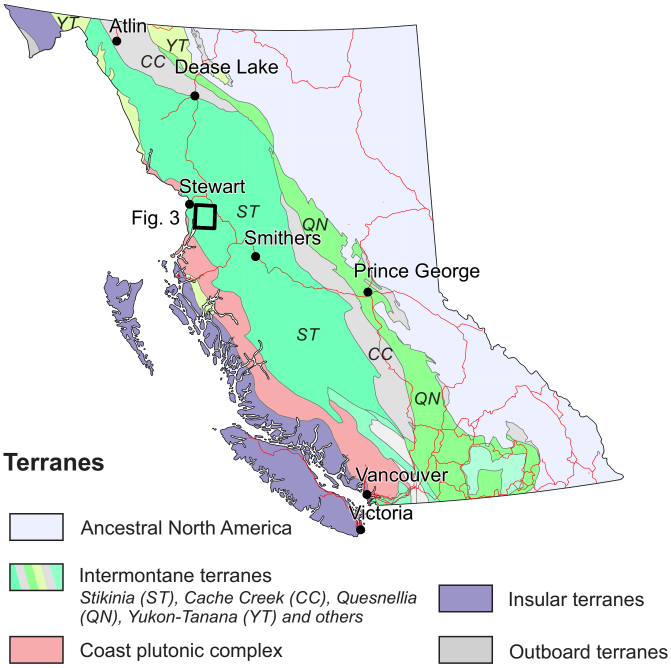

Fig. 1. Location of study area (after Nelson et al., 2013).

map data from north and east of Kinskuch Lake; 2) define volcano-sedimentary facies of the Hazelton Group in these sections and offer general environmental interpretations; 3) provide four preliminary U-Pb zircon and two $^{40}Ar/^{39}Ar$ ages; 4) compare Hazelton Group rocks in the Kitsault River area to those farther north in the Stewart-Iskut region such as described by Nelson et al. (2018); and 5) consider the implications for mineralizing systems in the area.

2. Geological setting

The Kitsault River study area is along the west-central margin of Stikinia, in the Intermontane belt of the Canadian Cordillera (Fig. 1). It lies in a belt of Triassic and Jurassic rocks that is bounded to the west by Eocene quartz monzonite to granodiorite of the Coast Plutonic Complex (Figs. 2, 3) and to the east by the Bowser basin (Middle Jurassic to Cretaceous; Fig. 3; Dawson and Alldrick, 1986). Terranes of the Intermontane belt (Slide Mountain, Yukon-Tanana, Quesnel, Stikine, Cache Creek, and Bridge River) were largely accreted to the western margin of Laurentia during the Jurassic and Triassic (Coney et al., 1980; Monger et al., 1982; Monger et al., 1991; Wheeler et al., 1991, Colpron et al., 2007; Nelson et al., 2013). Stikinia is a polyphase island arc terrane made up of the Stikine assemblage (Devonian to Mississippian; Anderson, 1989; Greig, 1992; Logan et al., 2000), the Stuhini and Takla groups (Middle to Late Triassic; Monger, 1977; Brown et al., 1996), and the Hazelton Group (latest Triassic to Middle Jurassic; Marsden and Thorkelson, 1992; Gagnon et al., 2012; Nelson et al., 2018).

The Stuhini Group preserves arc-related strata consisting of augite-rich basalt to basaltic andesite, crystal-lithic lapilli tuff, and epiclastic strata including greywacke, siltstone, tuff, and limestone units (Brown et al., 1996). The Hazelton Group overlies the Stuhini Group and older rocks largely along a regional unconformity (Greig, 2014; Nelson and Kyba, 2014). The Hazelton Group is an extensive package of volcanic and sedimentary rocks that span the entire width of the Stikine terrane (Marsden and Thorkelson, 1992; Gagnon et al., 2012; Nelson et al., 2018). It is subdivided into a lower part consisting mainly of siliciclastic rocks of the Jack Formation (which includes the Snippaker unit), and andesitic and lesser felsic volcaniclastic rocks of the Klastline and Betty Creek formations (Nelson et al., 2018 and references therein). The upper part of the Hazelton Group comprises mainly sedimentary rocks of the Spatsizi and Quock formations, subaerial dacite and rhyolite flows of the Mount Dilworth Formation, and bimodal volcanic and sedimentary rocks of the Iskut River Formation (Nelson et al., 2018). VMS-type mineralization is hosted in carbonaceous mudstone and rhyolites of the Iskut River Formation at the Au-Ag-rich Eskay Creek deposit (Barrett and Sherlock, 1996; Childe, 1996; MacDonald et al., 1996a; Roth et al., 1999; Barresi et al., 2015) and in inferred Iskut River Formation equivalent mafic volcanic and sedimentary rocks at the Cu-rich Anyox deposits (Smith, 1993; MacDonald et al., 1996b; Evenchick and McNicoll, 2002).

Overlying the Hazelton Group are widespread upper Middle Jurassic to mid-Cretaceous, marine and nonmarine sandstones, siltstones, and conglomerates of the Bowser Lake Group (Tipper and Richards, 1976; Eisbacher, 1981; Evenchick and Thorkelson, 2005; Evenchick et al., 2007). Post-Jurassic intrusive rocks in the Kitsault River area include the Ajax quartz monzonite (ca. 55.1 ±3 Ma, K-Ar; Carter, 1981; Dawson and Alldrick, 1986), quartz monzonite to granodiorite of the Coast Mountains Batholith (ca. 43 to 51 Ma; Carter, 1981) and inferred Eocene and younger microdiorite, diorite and lamprophyre dikes (Dawson and Alldrick et al., 1986; Devlin, 1987).

3. Notable mineral deposits in the Kitsault area

The study area is in the southern part of 'Golden Triangle', the popular name for a loosely defined region that includes most of the major gold, silver, and copper deposits in west-central Stikinia (Fig. 2). Notable deposits in the immediate study area include Homestake Ridge and Dolly Varden (Figs. 2, 3).

3.1. Homestake Ridge (MINFILE 103P 216)

The Homestake Ridge deposit (Figs. 2, 3) consists of the Homestake main, Homestake silver and South reef zones, with total Indicated resources of 0.624 Mt at 6.25 g/t Au, 47.9 g/t Ag and 0.18% Cu and Inferred resources of 7.245 Mt at 4.0 g/t Au, 90.0 g/t Ag and 0.11% Cu (Ross and Chamois, 2017). Volcanic rocks of the Hazelton Group host pyrite-chalcopyrite-galena-sphalerite mineralization in tabular zones of silica±carbonate±sericite±chlorite alteration, quartz veins, and quartz-carbonate hydrothermal breccias (Swanton et al., 2013; Ross and Chamois, 2017). West of the deposit area, across a thrust fault, sedimentary rocks (Stuhini Group) and andesitic volcanic

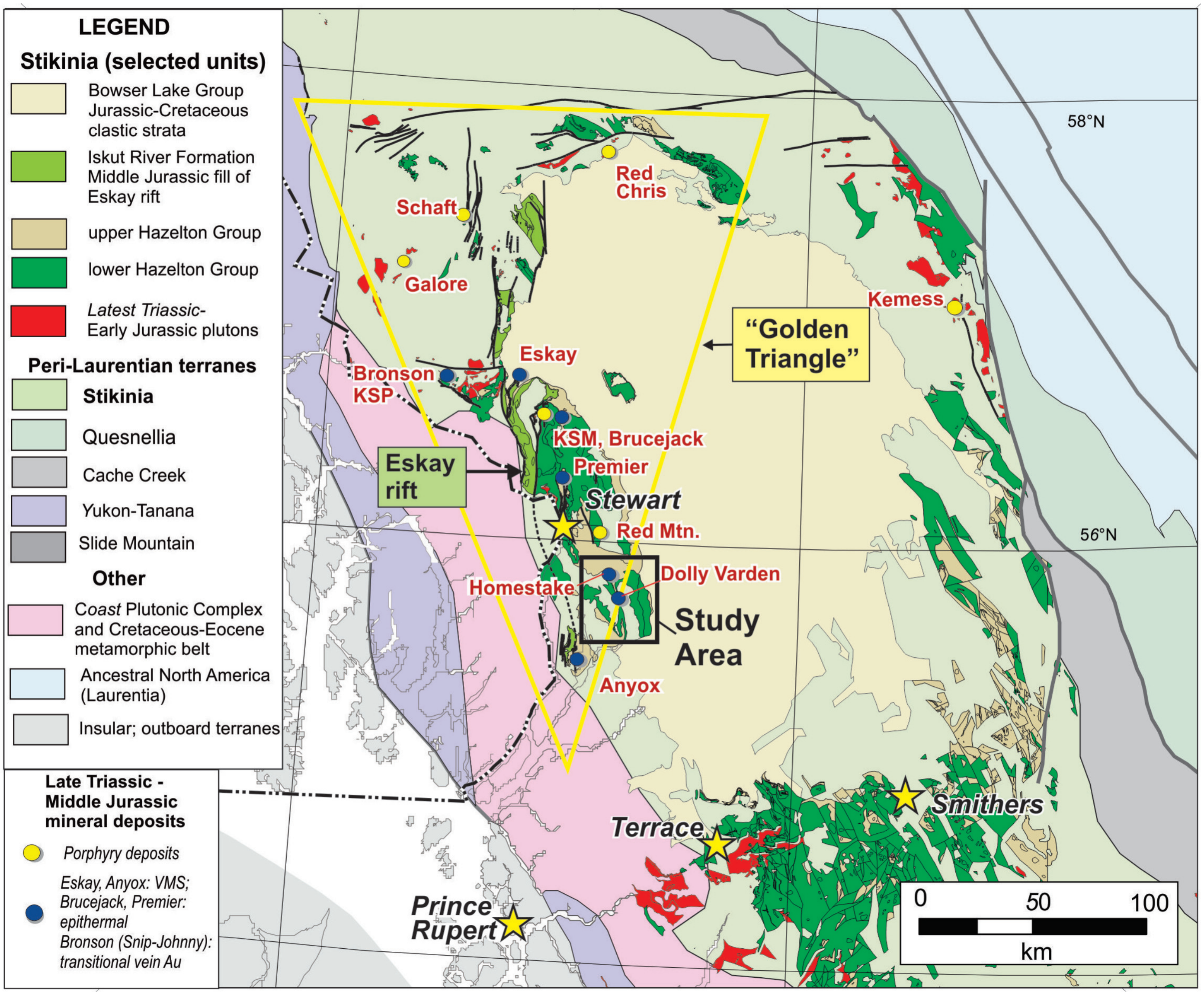

Fig. 2. Kitsault River study area with respect to major Late Triassic to Middle Jurassic mineral deposits in northwestern Stikinia (after Nelson et al., 2018).

rocks (Hazelton Group) are cut by numerous equigranular hornblende monzonite to hornblende-feldspar porphyritic dikes, and widespread quartz-pyrite±sericite±chlorite alteration locally obscures original protolith textures (Swanton et al., 2013). In contrast, the deposit area lacks monzonite dikes, aerially extensive alteration, and is underlain by Hazelton Group rocks, observations used by Swanton et al. (2013) to suggest that the western area may represent the deeper part of a hydrothermal system. Swanton et al. (2013) considered that the dikes west of the deposit area span the timing of alteration and suggested that they may be coeval with mineralization at Homestake Ridge. Below we report a new U-Pb zircon (CA-TIMS) age of ca. 191 Ma from a monzonite dike sampled near the Homestake Ridge deposit.

3.2. Dolly Varden, Torbrit, North Star, and Wolf (MINFILE 103P 188, 189, 191, 198)

The Dolly Varden Silver Corp. property contains the historical Dolly Varden, North Star, Torbrit, and Wolf deposits (Fig. 2), with total Indicated resources of 3.417 Mt at 299.8 g/t Ag and Inferred resources of 1.285 Mt at 277.0 g/t Ag (Turner and Nicholls, 2019). Between 1919 and 1959 the property produced approximately 20 Moz of silver (Dawson and Alldrick, 1986). Lithogeochemical studies throughout the Dolly Varden property suggest the volcanic country rocks are calc-alkaline (Sebert and Ramsay, 2012).

The Dolly Varden (MINFILE 103P 188), Torbrit (MINFILE 103P 191), and North Star (MINFILE 103P 189) deposits are described as exhalative and stratiform to locally vein-hosted silver-zinc-lead-barite orebodies underlain by andesitic crystal tuff and overlain by andesitic tuff of the Hazelton Group

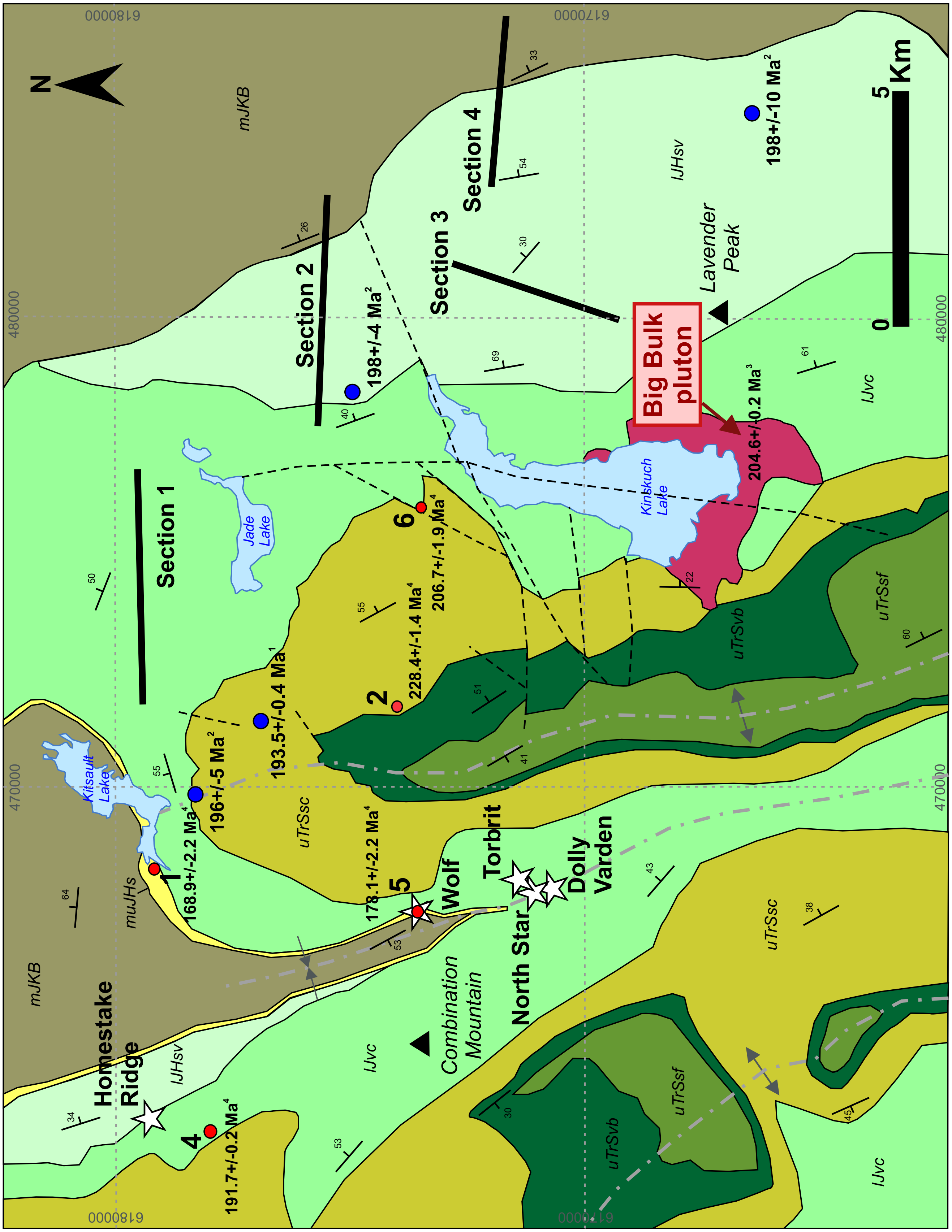

Fig. 3. Simplified geology of the Kitsault River area (after Alldrick et al., 1986; MacIntyre et al., 1994; Miller et al., 2020). Sources of geochronology: [1]Mortensen and Kirkham (1992); [2]Greig and Gehrels (1995); [3]Miller et al. (2020); [4]this study.

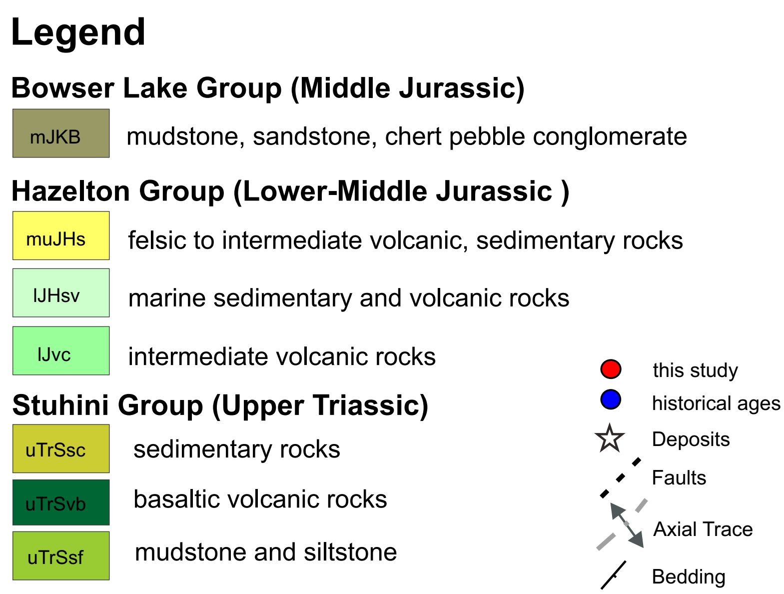

Fig. 3. Continued.

(Black, 1951; Campbell, 1959; Devlin, 1987, Higgs, 2015, McCuaig and Sebert, 2017). The Dolly Varden deposit is from 1 to 9 m thick and is divided into an east- to northeast-striking East Segment, and a west- to northwest-striking West Segment. Sulphide minerals at Dolly Varden East consist of pyrite, minor chalcopyrite, and trace argentite, pyrargyrite, and native silver disseminations and massive accumulations in white quartz veins (MINFILE 103P 188 and references therein). The Dolly Varden West mineralization is made up of sphalerite and galena, and minor pyrite, chalcopyrite, and tetrahedrite, with trace native silver as bands, disseminations, and stringers in calcite, quartz, siderite and barite gangue (MINFILE 103P 188 and references therein; Devlin, 1987).

The Torbrit deposit is hosted in rocks that have undergone propylitic, silica, and carbonate alteration, which extends approximately 30 m away from the ore zone (MINFILE 103P 191 and references therein). The mineralization consists of pyrite, sphalerite, and galena, with lesser chalcopyrite and trace pyrargyrite, argentite, and tetrahedrite interlaminated with brecciated quartz, calcite, barite, hematite, jasper, siderite, magnetite, and chlorite (MINFILE 103P 191 and references therein; Devlin, 1987). Locally, the Torbrit mineralization is formed together with colloform to crustiform banding and bladed open-space vein-filling textures (Higgs, 2015).

The North Star deposit shares many similarities with the Dolly Varden and Torbrit deposits and consists of bands, disseminations, and stringers of sphalerite and galena, minor pyrite, chalcopyrite, and tetrahedrite, and trace native silver and pyrargyrite hosted in calcite, quartz, siderite and barite exhalite (MINFILE 103P 189 and references therein). The deposit extends for about 100 m, is 1 to 24 m wide, and is cut by steeply dipping northwest-striking faults (MINFILE 103P 189 and references therein).

The Wolf deposit (MINFILE 103P 198) consists of several tabular mineralized zones. The No. 2 and No. 3 zones are the largest and are interpreted to be fault offset portions of the same body (Sebert and Ramsay, 2012). Sulphide minerals include pyrite, sphalerite, ruby silver, galena, tetrahedrite and possibly argentite in a gangue of banded and brecciated quartz±carbonate with open-space filling textures, including colloform banded quartz and pyrite, crustiform quartz, hematite, and bladed carbonate (Sebert and Ramsay, 2012). Pervasive chlorite-sericite alteration is common near the Wolf deposit, and silica, K-feldspar and Fe-carbonate alteration is close to the mineralized zones (Sebert and Ramsay, 2012). The No. 2 and No. 3 zones appear to be discordant to bedding and are interpreted to have been emplaced along an originally shallowly dipping fault; other mineralized zones may be concordant to bedding (Sebert and Ramsay, 2012). Although epigenetic textures predominate, possible local clastic sulphides and the presence of altered and mineralized clasts may suggest a syngenetic component (Sebert and Ramsay, 2012). Most of the tabular mineralized zones are close to the contact between intermediate tuff breccia and lapilli tuff and overlying intermediate lithic and/or crystal-rich volcaniclastic rocks. Limited fluid inclusion studies of the Wolf veins suggest formation at ~5 bar, implying moderate water depths (<50 m) or shallow burial by sedimentary-volcanic cover (<20 m) and formation in a near-surface setting (Dunne and Pinsent, 2002). Previous Pb isotope data from the Wolf deposit and other Dolly Varden deposits suggested a Jurassic depositional age (Godwin et al., 1991) but did not distinguish between the earliest part of the Early Jurassic (coeval with the lower Hazelton Group) or youngest part (Toarcian, coeval with the upper Hazelton Group). Below we present a new U-Pb zircon crystallization age (LA-ICPMS) of ca. 178 Ma from a felsic lapilli tuff sampled directly beneath the Wolf deposit indicating that these rocks are in the upper part of the Hazelton Group.

4. Geology of the Kitsault River area

Previous mapping in the region was by McConnell (1913), Turnbull (1916), Hanson (1922, 1923, 1928), Black (1951), Carter (1981), Alldrick et al. (1986), Dawson and Alldrick (1986); Grove (1986), Greig (1991); Greig et al. (1994); and Evenchick et al. (2008). Six informal stratigraphic units were recognized by Alldrick et al. (1986); Dawson and Alldrick (1986) and Greig (1991), including: 1) a 'lower sedimentary unit' of interbedded black siltstone, argillite, feldspathic wacke, and rare augite porphyritic basalt and hornblende porphyritic andesite; 2) a 'mafic volcanic unit' of augite, feldspar, and olivine basalt flows, pyroclastic rocks, conglomerates, and local limestones; 3) a 'middle sedimentary unit' of siltstone, sandstone, greywacke, conglomerate, and volcanic breccia containing limestone clasts; 4) an 'intermediate volcanic unit' of andesitic pyroclastic rocks (lapilli tuff to tuff breccia), and lesser lenses of argillite, limestone, chert and barite; 5) an 'epiclastic and felsic volcanic unit' of volcanic breccia, conglomerate, lesser dacite flows, pyroclastic rocks, minor siltstone and limestone, and local hornblende-feldspar porphyry flows; and 6) an 'upper sedimentary unit' of fossiliferous greywacke with belemnites and bivalves, black siltstone, sandstone, limestone, and arkose.

Previous Hazelton Group geochronology in the area includes U-Pb zircon ages of 193.5 ±0.4 Ma (Mortensen and Kirkham, 1992) and 196 ±5 Ma (Greig and Gehrels, 1995) from feldspar-phyric lapilli tuffs near Kitsault Lake (Fig. 3), and 198 ±4 Ma from K-feldspar- and plagioclase-phyric dacite-andesite flows north of Kinskuch Lake and 198 ±10 Ma from feldspar-phyric lapilli tuff to tuff breccia east of Lavender Peak (Fig. 3; Greig and Gehrels, 1995).

5. Stratigraphy and facies analysis

We present four composite stratigraphic sections based on 2019 mapping north of Kitsault Lake (Figs. 3, 4). These sections include the previously recognized (see above) unit 4 ('intermediate volcanic unit'; Lower to Middle Jurassic), unit 5 (epiclastic and felsic volcanic unit'), and unit 6 ('upper sedimentary unit'; Middle to Upper Jurassic). Given that volcano-sedimentary depositional systems generate environments that are repeated in time and space (e.g., Orton, 1995), below we adopt a facies approach to describe these rocks. Classification diagrams of Fisher (1966), Dott (1964), and Schmid (1981) were used to describe the pyroclastic and epiclastic rocks.

5.1. Lower part of the Hazelton Group

5.1.1. Facies 1; hornblende-plagioclase-phyric pyroclastic and epiclastic facies

Facies 1 was observed at section 1, where it is repeated, and at section 2 (Fig. 3). It is 1000 to 2500 m thick, but lower and upper contacts were not observed. Facies 1 consists mainly of poorly-sorted lapilli tuff to tuff breccia with subrounded to subangular hornblende-plagioclase-phyric clasts in a hornblende-plagioclase-crystal-bearing matrix (Fig. 5a). Limestone clasts, and partially to entirely weathered-out pits inferred to have been limestone clasts, are present locally. Some outcrops have m-scale hornblende- plagioclase-phyric blocks and accessory clasts of limestone and chert in a feldspar crystal-bearing matrix. Intercalated with the previously described units are minor m-scale coarse-grained tuff , limestone, feldspathic wacke, limestone clast-bearing lapillistone (Fig. 5b), and rare chert. A 10 m thick, green-weathering lapilli tuff to tuff breccia is in the central part of the facies. It consists of matrix-supported, poorly sorted, 0.1-1.0 cm subangular white aphyric possible felsic clasts, pink pumice lapilli, and 1-3% hornblende crystals (0.5-2 mm) in a tuff matrix (Fig. 5c). Near the top of the facies are 50-100 m thick beds of biotite-bearing, matrix- to clast-supported lapilli tuff to tuff breccia with subrounded to subangular 3 mm to 10 cm biotite- plagioclase-phyric clasts in a biotite and plagioclase crystal-bearing matrix (Fig. 6). It is interbedded with more recessive intervals consisting of feldspathic wacke. Near the base of facies 1 (Fig. 4), a 5 m thick, coherent, augite-plagioclase-phyric unit is present within lapilli tuff to tuff breccia and is inferred to be a sill.

5.1.2. Facies 2; epiclastic facies

The epiclastic facies was observed at section 1 and has an approximate thickness of 1500 m (Fig. 4). Contacts with facies 1 are gradational and are characterized by an increased proportion of epiclastic units adjacent to the facies 2 contact. Facies 2 consists of 50-100 m thick recessive beds of siltstone and fine-grained feldspathic sandstone in repeating fining upward sequences with 10-50 m-thick muddy limestone, feldspathic sandstone, conglomerate and rare chert all interbedded with competent 50-200 m-thick lapilli tuff to tuff breccia with local limestone clasts, and local plagioclase crystal-rich tuff. Interbeds of plagioclase crystal-rich tuff to lapilli tuff are moderately well-bedded, display weak grading and local 10-30 cm thick cross stratification (Fig. 7a). Interbedded 1-3 m thick conglomerates contain abundant maroon, gray, and white chert clasts, in addition to tuffaceous and hornblende-plagioclase-phyric clasts (Fig. 7b). Facies 2 includes minor 5-10 m-scale interbeds of lapilli tuff to tuff breccia with subrounded hornblende-plagioclase-phyric clasts in a hornblende and plagioclase crystal-bearing matrix.

5.1.3. Facies 3; hornblende-plagioclase-phyric volcanic facies

Facies 3 was observed at sections 2, 3, and 4 and is 250 to 1500 m thick (Fig. 4). Contact relationship with facies 1 were not observed; at the tops of sections 2 and 4, it appears to be in fault contact with rocks we consider part of the Bowser Lake Group. Facies 3 is subdivided into two distinct sub-facies (3a and 3b), which appear to be localized to the areas northeast and east of Kinskuch Lake. Facies 3 is a thick to very thick bedded, hornblende-plagioclase lapilli tuff, lapillistone, tuff breccia and pyroclastic breccia. It contains large (0.4 to 60 cm), subangular to subrounded, moderately to poorly sorted clasts in a fine- to coarse-ash matrix containing 2-5% hornblende

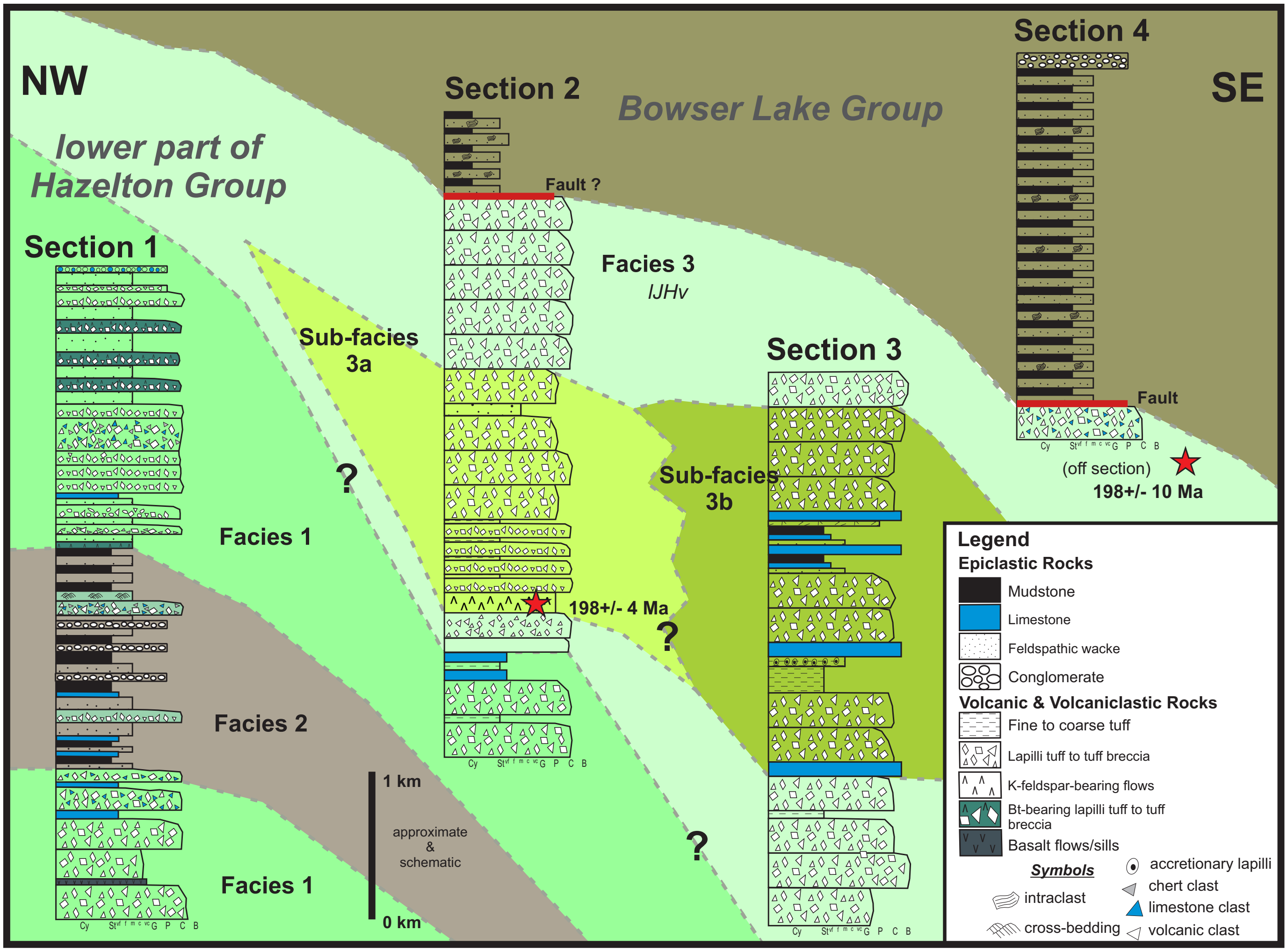

Fig. 4. Simplified composite stratigraphic sections based on map data in the Kitsault River area outlining three volcano-sedimentary facies and two sub-facies in the lower part of the Hazelton Group and their interpreted correlations. U-Pb zircon ages are from Greig and Gehrels (1995). See Figure 3 for section locations.

and abundant plagioclase crystals (Fig. 8a). Clasts are predominantly volcanic-derived hornblende- and plagioclase-phyric (1-5 mm) with varying phenocryst percentages (3-20%); the unit includes lesser aphyric clasts and rare limestone clasts. The unit varies from matrix- to clast-supported and is ungraded to weakly graded. Clasts have a range of colours including cream, gray, pink, brown, white and maroon and locally have cuspate to serrated edges. Up to 1 m thick, irregular and laterally-discontinuous beds of graded coarse- to fine-tuff locally separate layers of lapilli tuff to tuff breccia. Interbeds of maroon, thick-bedded, largely monomictic, matrix-supported lapilli tuff to tuff breccia are locally developed (Fig. 8b). These beds are poorly sorted, with uniform feldspar-phyric clasts that display irregular to wispy cuspate-lobate clast boundaries (suggesting they were still hot and ductile when deposited) in a fine-grained feldspar crystal and tuff matrix. Local rounded to subrounded hornblende-plagioclase-phyric bombs are in the largely monomictic beds. The U-Pb zircon age of 198 ±10 Ma reported by Greig and Gehrels (1995) for a feldspar-phyric lapilli tuff to tuff breccia seems to have been from a sample collected from facies 3 south of section 4.

5.1.3.1. Sub-facies 3a; K-feldspar and plagioclase porphyry

Sub-facies 3a is a distinct K-feldspar, hornblende, and plagioclase porphyry to crystal tuff observed northeast of Kinskuch Lake and in a small (~5 m) localized area north of Lavender Peak. It has a total thickness of approximately 1000 m and is interbedded with 100 m-thick units of hornblende-plagioclase-phyric lapilli tuff to tuff breccia (Fig. 4). Its contact appears conformable with underlying and overlying non-K feldspar-bearing facies 3. It varies in texture from massive, to flow-banded coherent rock, to plagioclase- and K-feldspar-bearing crystal tuff with K-feldspar crystals aligned along bedding (Fig. 9). These units are porphyritic with 2-5 mm plagioclase (2-5%) phenocrysts and locally 1-3 cm phenocrysts of K-feldspar (1-3%). The unit contains quartz (1-3%), hornblende (5-10%), plagioclase (10-20%), and K-feldspar (70-85%). The feldspar porphyry to crystal tuff is interbedded

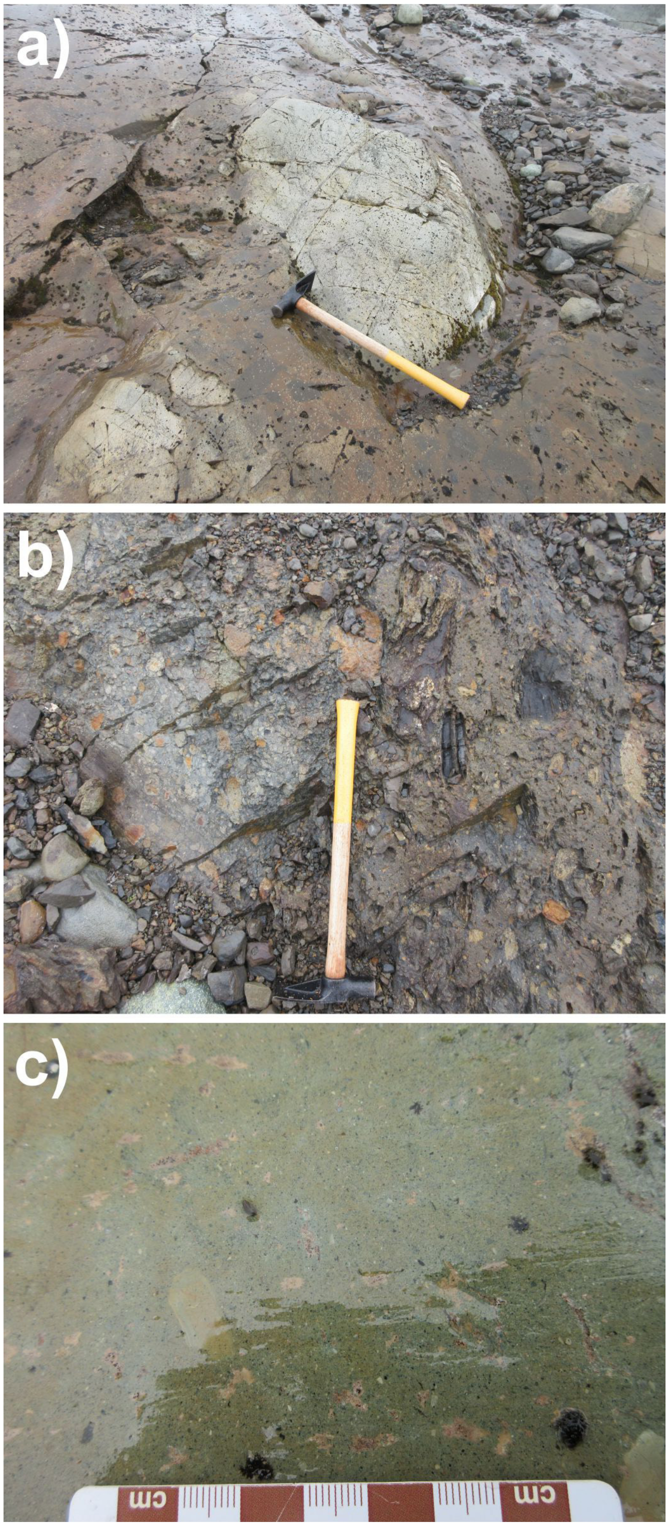

Fig. 5. Lapilli tuff to tuff breccia unit of facies 1. **a)** Angular m-scale hornblende-plagioclase volcanic clasts in a thick-bedded tuff breccia unit (UTM 474981E; 6179756N). **b)** Clast-supported lapillistone with plagioclase-phyric volcanic and limestone clasts (UTM 476634E; 6179605N). **c)** Distinct green-weathering polymictic lapilli tuff with cream to black aphanitic angular clasts and ameboid vesicular pumice clasts floating in a fine-grained plagioclase-rich matrix (UTM 474541E; 6179496N).

Fig. 6. Lower Hazelton Group facies 1, matrix-supported lapilli tuff with poorly sorted subangular biotite-hornblende-plagioclase-phyric clasts in a biotite-plagioclase matrix (UTM 475438E; 6179368N).

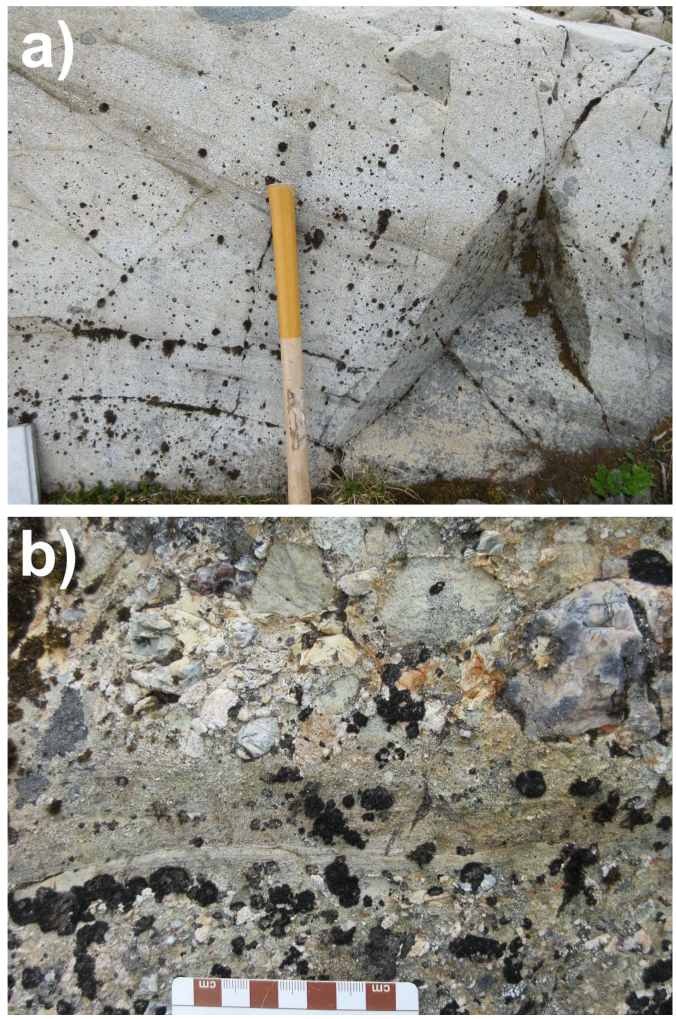

Fig. 7. Lower Hazelton Group facies 2, epiclastic units. **a)** Cross-stratified and parallel-stratified plagioclase crystal-rich tuff (UTM 473730E; 6179381N). **b)** Beds of clast- to matrix-supported polymictic conglomerate with rounded to subrounded clasts of chert, fine-grained tuff, and various plagioclase porphyritic fragments separated by a volcanic-derived sandstone layer (UTM 474247E; 6179466N).

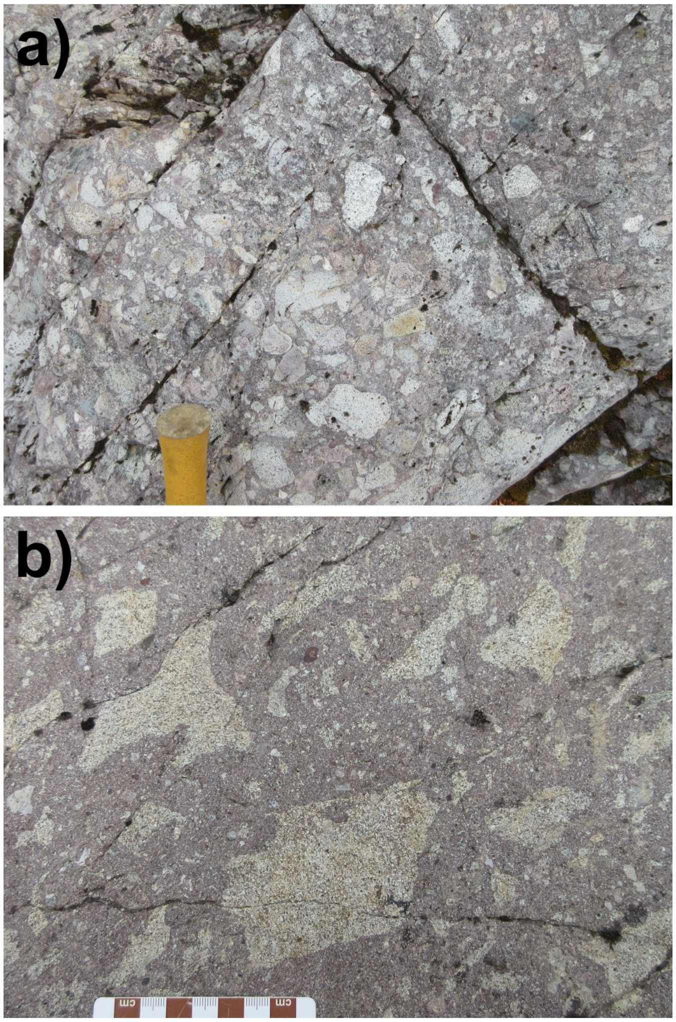

Fig. 8. Lower Hazelton Group facies 3, volcaniclastic rocks. **a)** Clast-supported lapillistone to lapilli tuff with subrounded to subangular hornblende-feldspar-phyric clasts with variable hornblende/ plagioclase percentages (UTM 479119E; 6172627N). **b)** Largely monomictic lapilli tuff with crowded, coarse-grained plagioclase-phyric clasts with lobate-cuspate margins in a feldspar-phyric maroon tuff matrix containing local subrounded dark maroon fine-grained clasts (UTM 479084E; 6172610N).

with gray to maroon lapilli tuff to tuff breccia with 1-20 cm subrounded hornblende-plagioclase-phyric clasts (phenocryst percentages vary from 3-25%) in a hornblende and plagioclase crystal matrix. Weakly graded, thin- to medium-bedded, coarse- to fine-tuff interbeds are present locally. Lenticular and discontinuous beds of brown weathering, coarse- to very coarse-grained sandstone, 3-5 m thick are interlayered with the feldspar porphyry and lapilli tuff to tuff breccia units. Greig and Gehrels (1995) reported a 198 ±4 Ma zircon U-Pb age for a K-feldspar/plagioclase-phyric dacite/andesite sample collected in sub-facies 3a along section 2 (Fig. 4).

5.1.3.2. Sub-facies 3b; hornblende-plagioclase-phyric volcanic rocks, tuff and limestone

At section 3, sub-facies 3b conformably overlies facies 3 rocks

Fig. 9. Lower Hazelton Group facies 3a, hornblende-plagioclase-K-feldspar porphyry with zoned K-feldspar crystals up to 3 cm long aligned along bedding (UTM 479658E; 6175426N).

and is about 2000 m thick (Fig. 3). The unit consists of lapilli tuff, lapillistone, and tuff breccia, and rocks such as limestone, limestone clast-rich conglomerate, fine-grained sandstone, and mudstone. The tuff unit consists of interbedded (1-20 cm scale) rhythmically laminated fine and coarse tuff and lapilli tuff with 1-3 mm aphyric, white to cream lapilli (Fig. 10a). M-thick beds of lapillistone containing 2-5 mm concentrically zoned aphyric accretionary lapilli in a coarse tuff matrix are locally developed (Fig. 10b). A local variety of lapilli tuff to tuff breccia contains characteristic sparse subrounded black, glassy lapilli fragments with 1-5% plagioclase phenocrysts floating in a feldspar-rich crystal matrix (Fig. 10c). These glassy lapilli and their feldspar-rich matrix form distinct 10-30 cm subrounded clasts in the same unit (Fig. 10d).

Calcareous mudstone and limestone form abundant 1-2 m thick beds in facies 3b. The limestone forms cm-scale lenses, discontinuous layers, and ovoid bodies in the calcareous mudstone (Fig. 11a). Parts of the sequence with abundant limestone also contains fine-grained sandstone and mudstone with well-developed grading and abundant load casts and flame structures and other soft-sediment deformation features (Fig. 11b) and minor beds of medium- to coarse-grained feldspathic sandstone.

5.2. Bowser Lake Group

5.2.1. Interbedded feldspathic wacke, mudstone, and chert clast-bearing pebble conglomerate

Interbedded gray to brown, laminated- to medium-bedded, fine- to medium-grained feldspathic wacke and mudstone (Fig. 12a) is present along the eastern margin of Kitsault River map area. Load and flame structures are well developed, and 1-5 cm subrounded mudstone intraclasts are observed throughout the unit. The chert-pebble conglomerate forms m-scale beds containing granules and pebbles in a coarse sandstone matrix (Fig. 12b). Clasts are subrounded and consist

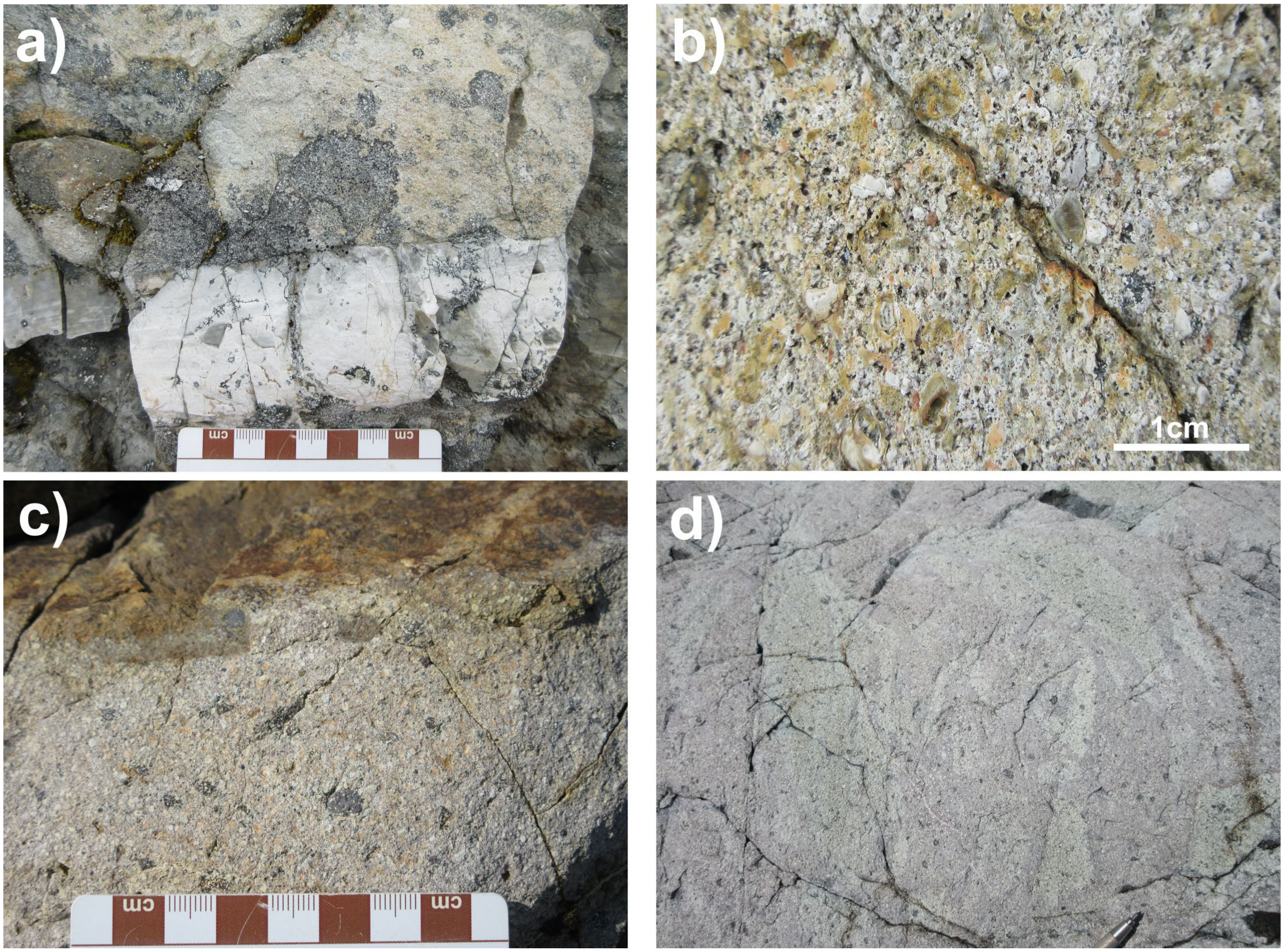

Fig. 10. Lower Hazelton Group facies 3b pyroclastic units. **a)** Dm-scale interlayers of light-toned rhythmically laminated fine tuff and dark-toned beds of coarse tuff, with internal thin layering (UTM 480620E; 6170990N). **b)** Clast-supported lapillistone with abundant accretionary lapilli (UTM 480620E; 6170990N). **c)** Sparse black, cm-scale rounded glassy lapilli fragments in plagioclase crystal matrix (UTM 480074E; 6169483N). **d)** Tuff breccia with tabular, aligned breccia- to lapilli-sized clasts, up to 10 cm, of similar composition to c) (UTM 480048E; 6169615N).

of white, tan, gray, and black chert. The conglomerate is interbedded with cm-scale gray siltstones.

6. Geochronology

Below we report the preliminary results from four Laser Ablation Inductively Coupled Plasma Mass Spectrometry (LA-ICPMS) U-Pb zircon samples, one Chemical Abrasion Thermal Ionization Mass Spectrometry (CA-TIMS) U-Pb zircon sample, and two $^{40}Ar/^{39}Ar$ K-feldspar samples collected during 2015 mapping (Fig. 3; Table 1). Our sample of hornblende diorite from a plutonic body on the southeast shore of Kinskuch Lake that hosts the Big Bulk porphyry Cu-Au prospect (see Miller et al., 2020) failed to yield adequate zircons for analysis. However, Miller et al. (2020) report a preliminary U-Pb zircon CA-TIMS age of from an early diorite phase at the property of 204.61 ±0.18 Ma.

Detailed methods and final results will be reported elsewhere. U-Pb zircon and $^{40}Ar/^{39}Ar$ K-feldspar analyses were carried out at the Pacific Centre for Isotopic and Geochemical Research

Table 1. Location and analysis information for reported 2015 geochronological samples. Coordinates are in UTM Zone 9N, NAD83.

Sample	Easting	Northing	Analysis
1	468325	6179294	U-Pb zrn detrital
2	471841	6174086	U-Pb zrn detrital
4	462704	6178223	U-Pb zrn TIMS igneous
5	467432	6173676	U-Pb zrn LA-ICP-MS igneous
6	476098	6173707	U-Pb zrn detrital
7	467257	6173616	Ar-Ar adularia
8	467312	6173724	Ar-Ar adularia

(University of British Columbia). For all LA-ICPMS analyses, we exclude individual grain ages with <0.05 probability of concordance (calculated using the Isoplot routine of Ludwig, 2012). We calculated preliminary maximum depositional ages for detrital zircon samples using: 1) the youngest graphical probability peak (YPP) in a probability density plot (PDP)

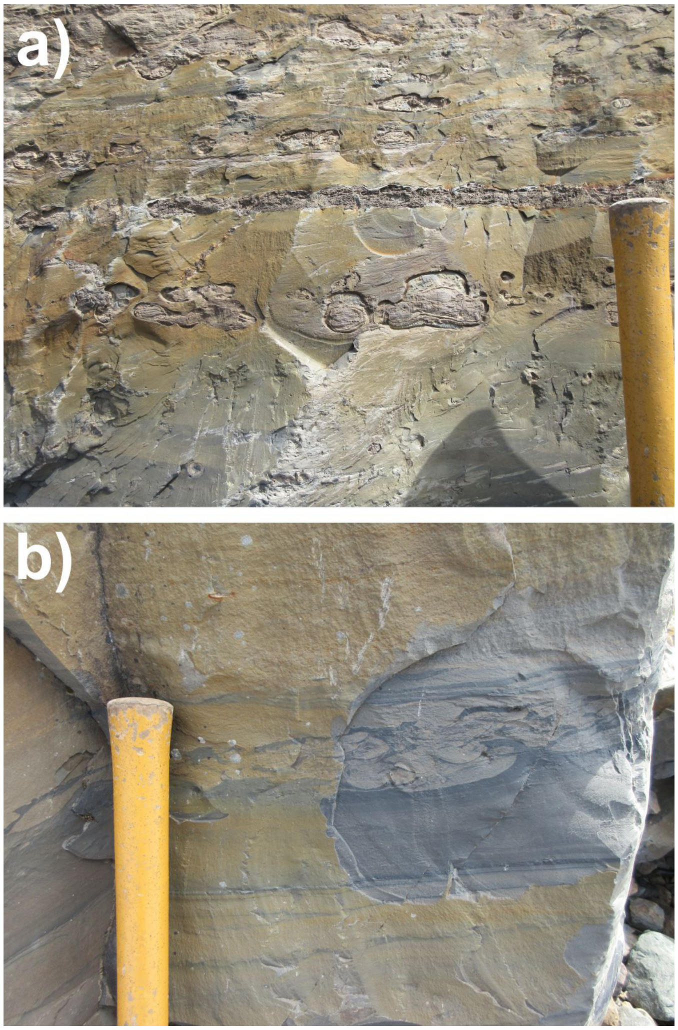

Fig. 11. Facies 3b epiclastic units. **a)** Laminated calcareous mudstone with cm-scale layers, lenses, and ovoid limestone bodies. **b)** Sharp-based fining upward sequences with graded fine-grained sandstone to mudstone; load casts and flame structures at top of hammer handle. Both units located at (UTM 480251E; 6171402N).

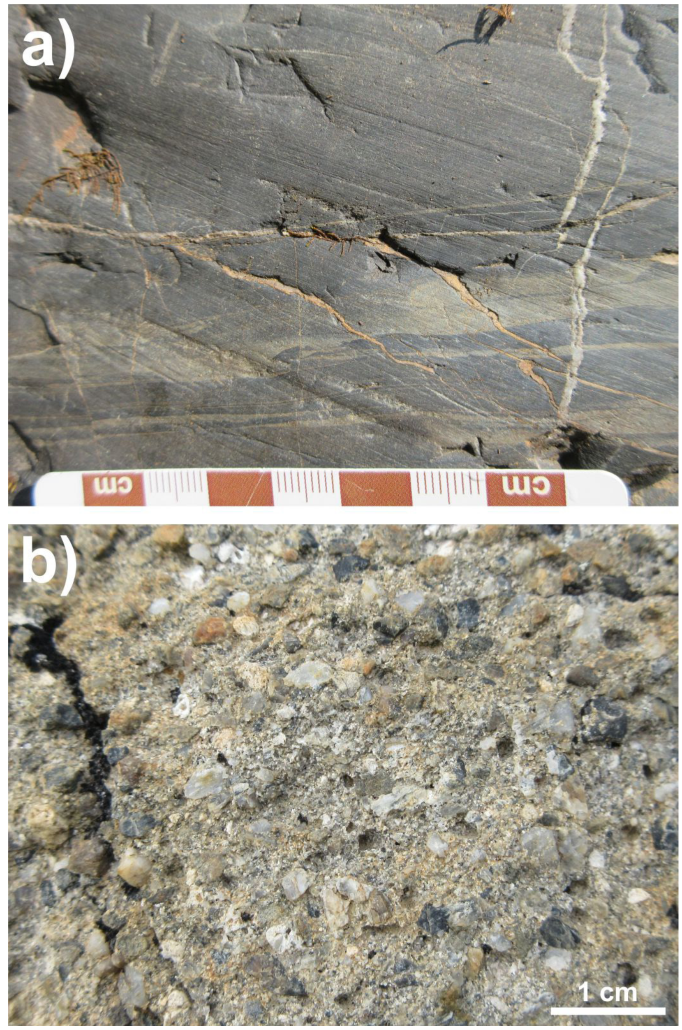

Fig. 12. Bowser Lake Group. **a)** Interlayered mudstone and siltstone (dark toned) and fine-grained sandstone (light toned) (UTM 482152E; 6175728N). **b)** Chert-granule pebble conglomerate in a very coarse-grained sandstone matrix (UTM 485798E; 6171726N).

constructed in Isoplot (Ludwig, 2012); 2) the youngest statistical population (YSP, Coutts et al., 2019); 3) the TuffZirc routine in Isoplot (Ludwig, 2012); and 4) the youngest cluster of two or more grains that overlap in age at 1 sigma (YC1σ(2+), Dickinson and Gehrels, 2009). Following Herriott et al. (2019) we choose YPP as the preferred preliminary maximum depositional age.

6.1. Lower part of the Hazelton Group

6.1.1. Sample 15BvS-37-08, detrital zircon from volcanic-derived sandstone (LA-ICPMS) This sample was collected from the base of the Hazelton Group northwest of Kinskuch Lake (Sample 2, on Fig. 3). It is from a well-stratified hornblende crystal-bearing and plagioclase crystal-rich volcanic-derived sandstone that is interbedded with argillite. The sandstone appears to unconformably overlie Stuhini Group argillite and chert containing limestone, augite-phyric volcanic, and chert megaclasts (see Miller et al., 2020). The sample returned a unimodal Late Triassic detrital zircon population, and the youngest statistical population yielded a 228.4 ±1.4 Ma preliminary maximum depositional age (Fig. 13d).

6.1.2. Sample 15BvS-36-13, detrital zircon from polymictic pebble conglomerate (LA-ICPMS)

This sample is from a polymictic pebble conglomerate containing clasts of hornblende-plagioclase-phyric volcanic rock, grey limestone, black chert, sandstone, conglomerate, and rare maroon plagioclase-phyric volcanic rock at the base of the Hazelton Group about 1 km northwest of Kinskuch Lake (Sample 6 on Fig. 3). This conglomerate is overlain by volcanic breccia with hornblende-plagioclase-phyric clasts interbedded with crystal tuff, typical of the lower part of the Hazelton Group throughout the Stewart-Iskut area. At this location, the polymictic pebble conglomerate appears to overlie Stuhini

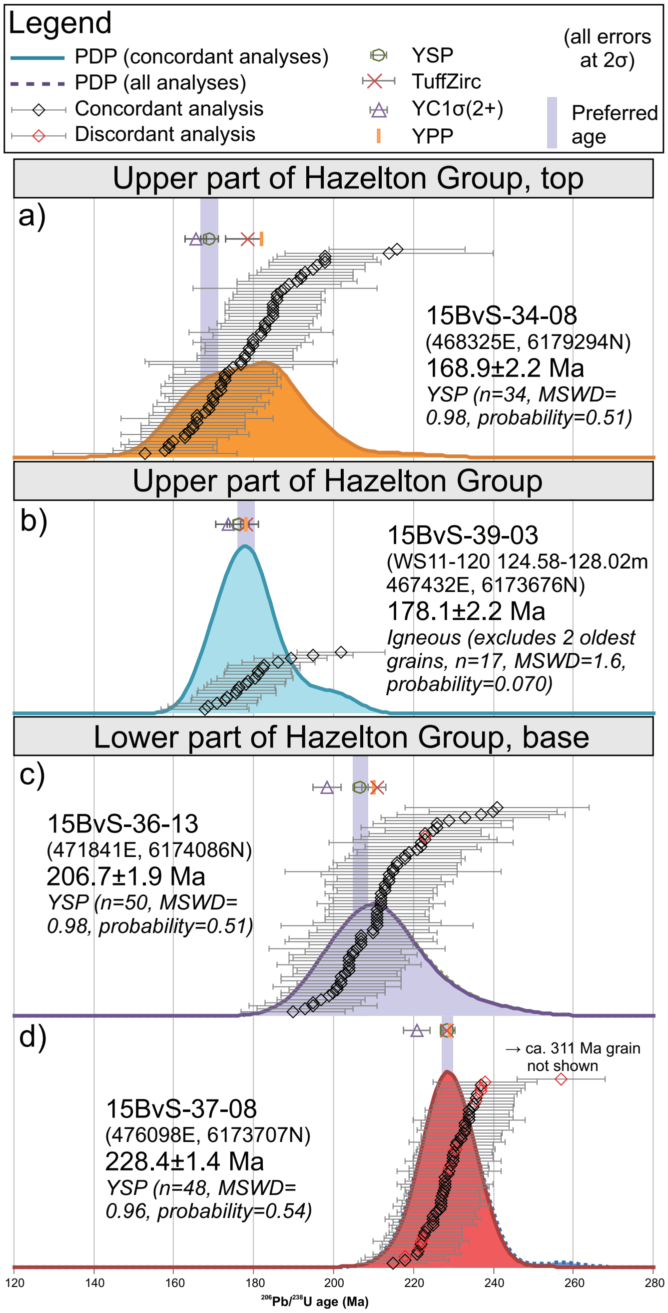

Fig. 13. LA-ICP-MS zircon $^{206}Pb/^{238}U$ probability density plot (PDP), individual grain ages, and preliminary maximum depositional or igneous age. **a)** Volcanic-derived sandstone bed in upper part of the Hazelton Group, immediately below the Quock Formation. **b)** Felsic lapilli tuff in the footwall of the Wolf deposit, upper part of the Hazelton Group. **c)** Polymictic pebble conglomerate at the base of the Hazelton Group. **d)** Volcanic-derived sandstone interbedded with argillite at the base of the Hazelton Group. Preliminary maximum depositional ages are constrained using the youngest graphical probability peak (YPP), youngest statistical population (YSP), TuffZirc, and youngest cluster of two or more grains that overlap in age at 1 sigma (YC1σ(2+)).

Group interstratified argillite, sandstone, and conglomerate without a marked discordance. The Stuhini Group conglomerate beds include augite-phyric volcanic clasts, plagioclase-phyric volcanic clasts, purple volcanic clasts, and argillite intraclasts, but lack hornblende-plagioclase-phyric volcanic and limestone clasts typical of conglomerates in the overlying lower Hazelton Group. The youngest statistical population returned a 206.7 ±1.9 Ma preliminary maximum depositional age (Fig. 13c).

6.2. Sample 15BvS-38-01, monzonite dike at the Homestake Ridge deposit area (CA-TIMS)

We sampled a variably-altered monzonite dike with locally well-preserved 3-7 mm blocky to tabular hornblende west of the Homestake Ridge deposit area (Sample 4 on Fig. 3). The dike cuts recessive interbedded argillite and fine-grained sandstone (likely part of the Stuhini Group). The sample returned a preliminary U-Pb zircon crystallization age of 191.71 ±0.20 Ma (Fig. 14).

6.3. Upper part of the Hazelton Group

6.3.1. Sample 15BvS-39-03, felsic lapilli tuff (LA-ICPMS)

This drill core (DDH WS11-120, 124.6-128.0 m downhole) sample is from the footwall of the Wolf No. 2 zone (Sample 5 on Fig. 3; Fig. 15; Sebert and Ramsay, 2012). It is from a lower sequence of tuffaceous sandstone and argillaceous tuff that is overlain by a section of intermediate lithic and/or crystal-rich volcaniclastic rocks (Sebert and Ramsay, 2012). The upper volcanic rock package is in turn overlain by argillite and calcareous sandstone that occupy the core of a syncline in the Kitsault River valley (Alldrick et al., 1986; Sebert and Ramsay, 2012). These argillites and calcareous sandstones were previously assigned to an undivided upper sedimentary unit (Alldrick et al., 1986) or the Salmon River Formation (Sebert and Ramsay, 2012). Following mapping to the north by Greig et al. (1994) and an updated regional stratigraphic framework by Nelson et al. (2018), we suggest that these rocks are best assigned to the Quock Formation (upper part

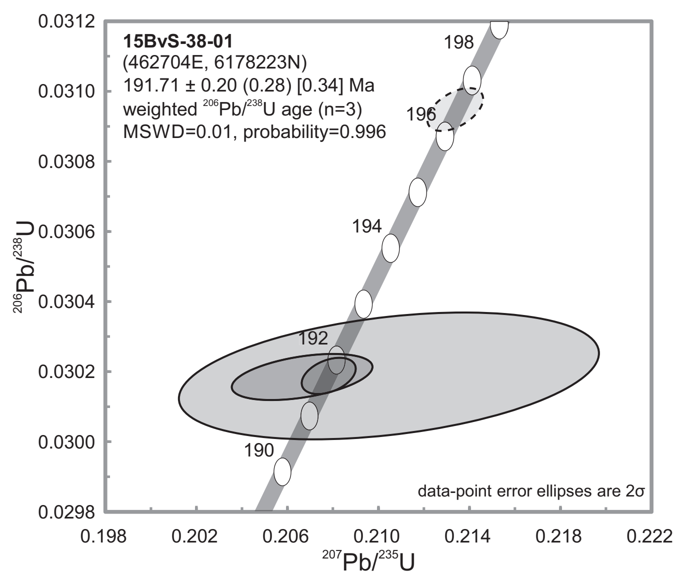

Fig. 14. U-Pb zircon concordia diagram showing CA-TIMS results from a hornblende monzonite dike west of the Homestake Ridge deposit.

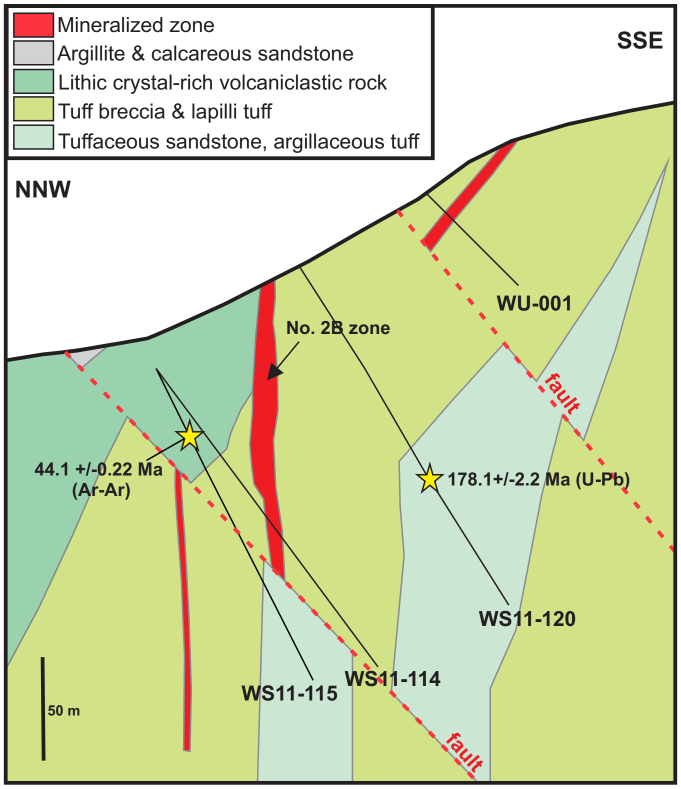

Fig. 15. Simplified schematic cross section through the Wolf deposit modified from sections 1250 N, 1300 N and 1350N in Sebert and Ramsay (2012). Ages are from this study.

of the Hazelton Group) and Bowser Lake Group. The sample returned a preliminary U-Pb zircon LA-ICPMS crystallization age of 178.1 ±2.2 Ma (Fig. 13b). Based on this age and stratigraphic position directly beneath sedimentary rocks of the Quock Formation or Bowser Lake Group, these rocks are best assigned to the upper part of the Hazelton Group.

6.3.2. Sample 15BvS-34-08, volcanic-derived sandstone (LA-ICPMS)

This sample was taken from near the southwest arm of Kitsault Lake (Sample 1 on Fig. 3). It is from a sandstone interval, about 8 m thick and containing common belemnite casts, that gradationally overlies volcanic rocks with cm-scale, light-coloured aphanitic to plagioclase-phyric felsic volcanic clasts. Both units are interpreted here as part of the upper Hazelton Group. The sandstones are overlain by a 65 m-thick succession of interstratified dark grey siltstone, pale grey siliceous siltstone, and fine felsic tuff of the Quock Formation (upper Hazelton Group), which is in turn is overlain by laminated to medium-bedded argillite, siltstone, and fine-grained feldspathic arenite of the Bowser Lake Group. The sample returned a unimodal, largely Early to Middle Jurassic detrital zircon population. The youngest statistical population yields a 168.9 ±2.2 Ma preliminary maximum depositional age, which accords well with a ca. 170 Ma shoulder on the probability density plot (Fig. 13a).

6.4. Hydrothermal alteration

6.4.1. Sample 15BvS-39-01, altered volcaniclastic rock, $^{40}Ar/^{39}Ar$ K-feldspar

This is a drill core sample from the Wolf deposit (sample 7, Fig. 3) taken from DDH WS11-108, 122.4-123.5 m downhole. The sample was taken approximately 63 m above (measured along the drill hole) mineralization at the No. 2 zone (Sebert and Ramsay, 2012). We analyzed a pale K-feldspar altered, generally massive, poorly-sorted volcaniclastic rock with minor matrix-supported, subrounded to subangular andesitic volcanic clasts in a crystal-rich matrix. The sample did not return a robust Ar-Ar K-feldspar plateau age (using criteria defined by Ludwig, 2012). However, combination of heating steps 7-9 yields a preliminary age of 44.23 ±0.43 Ma that includes 35.6% of ^{39}Ar (Fig. 16).

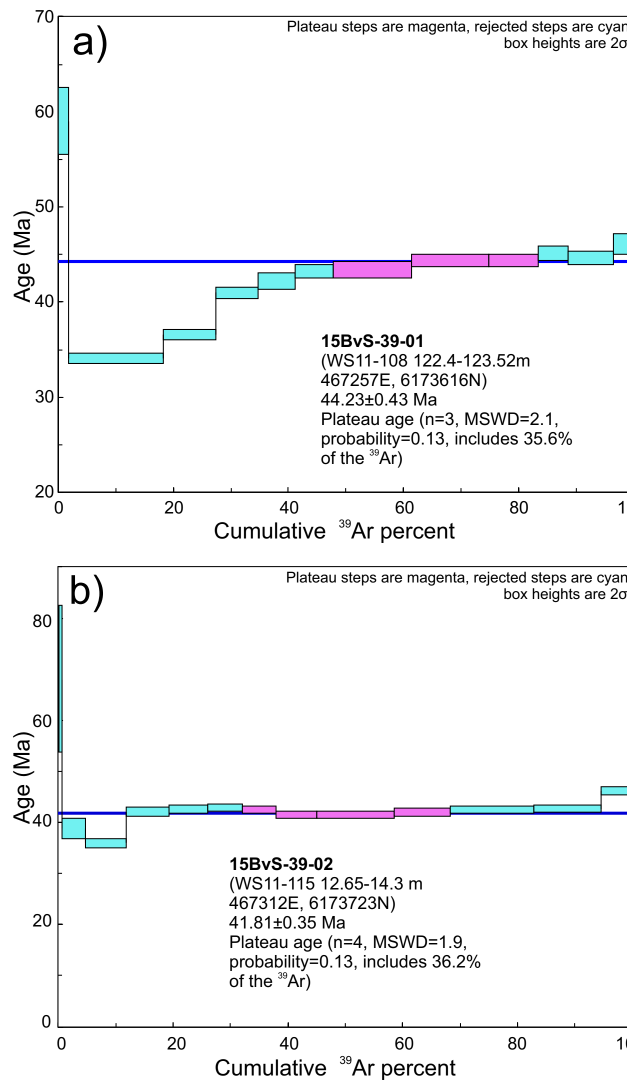

Fig. 16. Ar-Ar K-feldspar step-heating spectra from altered rocks at the Wolf deposit.

6.4.2. Sample 15BvS-39-02, altered volcaniclastic rock, $^{40}Ar/^{39}Ar$ K-feldspar

This is a drill core sample from the Wolf deposit (sample 8,

Fig. 3, Fig. 15), taken from DDH WS11-115, 12.7-12.9 m and 13.5-14.3 m downhole. The sample is about 21 m above (measured along the drill hole) mineralization at the No. 2B zone, which is at the contact between a unit of intermediate tuff breccia and lapilli tuff and an overlying unit of intermediate lithic and/or crystal-rich volcaniclastic rocks (Fig. 15; Sebert and Ramsay, 2012). We analyzed a K-feldspar-, sericite-, and locally Fe carbonate-altered, largely massive and poorly sorted volcaniclastic rock with matrix- to locally clast-supported subrounded to angular andesitic clasts in a crystal-bearing matrix. The sample did not return a robust Ar-Ar K-feldspar plateau age (using criteria defined by Ludwig, 2012). However, combination of heating steps 7-10 yields a preliminary age of 42.11 ±0.22 Ma that includes 36.2% of ^{39}Ar (Fig. 16).

7. Discussion

7.1. Preliminary environmental interpretations

Most of the lower Hazelton Group consists of lapilli tuff to tuff breccia with hornblende-plagioclase-phyric volcanic-derived clasts. Facies 1 consists mainly of coarse-grained pyroclastic rocks, indicating proximal-type explosive volcanism; m-scale intercalations of limestone and chert may indicate a subaqueous setting but abundant accessory limestone and chert clasts in pyroclastic rocks indicate coeval erosional stripping. Epiclastic rocks of facies 2 may mark a relative hiatus in volcanism. Abundant mudrocks with lesser muddy limestones and rare chert beds likely signify subaqueous sedimentation but polymictic conglomerates with well-rounded volcanic and chert clasts indicate intraformational erosion and subaerial and/or shallow-water reworking. Facies 3 also consists mainly of coarse pyroclastic rocks indicating proximal explosive volcanism; that some clasts with cuspate-lobate boundaries (suggesting ductility during emplacement) lack welding may signify subaqueous deposition. Sub-facies 3a is similar to facies 3 except that it contains abundant coarse-grained to megacrystic K-feldspar crystals and distinctly coherent and flow-banded textures. In facies 3b, the preservation of rhythmically laminated fine-grained sandstone to mudstone in sharp-based fining upward-sequences likely indicates mass flow sedimentation below fair-weather wave base. Sub-facies 3b also contains abundant limestone beds; local accretionary lapilli and glassy lapilli were likely derived from laterally adjacent subaerial eruptions (see e.g., McPhie et al., 1993).

7.2. Ages and regional correlations

Geochronology data presented above from the lower Hazelton Group yielded maximum depositional ages of 228.4 ±1.4 Ma (hornblende-plagioclase crystal-rich sandstone) and 206.7 ±1.9 Ma (polymictic pebble conglomerate). The detrital zircon population of the sandstone suggests derivation from erosion of Stikine plutonic suite sources (Late Triassic, ca. 229-216 Ma), similar to other detrital zircon samples from basal lower Hazelton Group throughout the Stewart-Iskut area (e.g., Nelson et al., 2018). The polymictic pebble conglomerate sample returned a unimodal Late Triassic to earliest Jurassic detrital zircon population, likely resulting from overlapping penecontemporaneous lower Hazelton Group volcanic sources (latest Triassic to earliest Jurassic). Deposition of the lower part of the Hazelton Group in the Kitsault River area was likely between ca. 206 Ma (Rhaetian) to ca. 196 Ma (Greig and Gehrels, 1995; Sinemurian).

The ca. 206 Ma volcanic-derived sandstone is potentially correlative to the Jack Formation (Nelson et al., 2018) of the southern Iskut Region and may similarly signify a break between the Hazelton Group rocks from the underlying Stuhini Group (Nelson et al., 2018). The ca. 196 Ma lapilli tuff to tuff breccias of facies 1 and 3, may be temporal equivalents to the Unuk River andesite unit described by Nelson et al. (2018). Predominantly epiclastic rocks of facies 2 are likely a local stratigraphic variation within the predominantly andesite unit. Sub-facies 3a (K-feldspar porphyritic unit) could be correlative to ca. 196 Ma porphyritic diorite (J. Nelson unpublished data, 2017) observed northwest of Brucejack Lake (Nelson et al., 2018). Alternatively, it may be related to the Brucejack Lake felsic unit, which is described as a felsic deposit, including K-feldspar-, plagioclase- and hornblende-phyric flows, breccias and bedded welded to non-welded tuffs (MacDonald, 1993). In the Brucejack area, this porphyritic unit has yielded a U-Pb age of ca. 183-188 Ma, which is younger than the ca. 196 Ma age from Grieg and Gehrels (1995).

The altered ca. 191 Ma monzonite dyke sampled west of the Homestake Ridge deposit is close to the ca. 196 Ma age (Greig and Gehrels, 1995) andesitic lapilli tuff to tuff breccia and K-feldspar porphyries. It is therefore possible that the Homestake Ridge mineralization is Early Jurassic. Felsic lapilli tuff in the footwall of the Wolf deposit in the Kitsault River valley west of our 2019 study area (Fig. 2) gave a crystallization age of 178.1 ±2.2 Ma (Toarcian), indicating that the area is underlain by the upper part of the Hazelton Group (Toarcian and younger). However, the bimodal mafic-felsic volcanic package characteristic of the similarly aged Iskut River Formation (Nelson et al., 2018) has not been observed in the Kitsault River valley.

Volcanic-derived sandstone with belemnite casts sampled near Kitsault Lake returned a preliminary maximum depositional age of 168.9 ±2.2 Ma, which suggests rocks temporally equivalent to the Quock Formation are present along the northern margin of the Kitsault River area and likely continue into the Kitsault River valley where the Dolly Varden deposits are located.

K-feldspar ^{40}Ar/^{39}Ar ages of ca. 42 and 44 Ma were interpreted from altered lapilli tuff units sampled above the Ag-rich mineralization at the Wolf deposit. K-feldspar, including both coarse- and fine-grained low-temperature polymorph adularia, has been successfully used to date epithermal deposits (e.g., Henry et al., 1997). The closure temperature of K-feldspar in the argon system ranges from 150-300°C and likely records late cooling histories, intermediate between ^{40}Ar/^{39}Ar biotite and apatite fission track data (Kelley, 2002; Streepey et al., 2002). We tentatively interpret the ca. 42-44 Ma ages record thermal perturbations and/or fluid flow associated with the formation of the Coast Plutonic Complex and related Eocene intrusions.

7.3. Implications for VMS-type mineralization systems of the Kitsault River area

VMS deposits form at or immediately beneath the seafloor in response to hydrothermal systems active during volcanism, and consist of syngenetic, stratabound, and locally stratiform lenses of massive sulphide and discordant vein- and/or stockwork-hosted sulphide (Large et al., 2001; Franklin et al., 2005; Galley et al., 2007). In the Kitsault River area, the lower part of the Hazelton Group hosts several high-grade Ag-Pb-Zn stratabound, vein- and breccia-hosted deposits, including the Dolly Varden, Torbrit and North Star mines that were active between 1915 and 1959 (Hanson, 1922; Black, 1951; Campbell, 1959; Dawson and Alldrick, 1986; Devlin and Godwin, 1986; Pinsent, 2001; Dunne and Pinsent, 2002). These deposits lie well to the east of the main Eskay rift trend (Fig. 2). The Ag-Pb-Zn mineralization in the Kitsault River area has been variably interpreted as epithermal vein-related (Grove, 1986), stratiform VMS (Devlin and Godwin, 1985; Devlin, 1987) or related to shallow subaqueous hot springs (Dunne and Pinsent, 2002). Our new age of ca. 178 Ma shows this mineralization is cogenetic with precious and base metal-rich VMS deposits hosted in the upper part of the Hazelton Group elsewhere, such as at Eskay Creek and Anyox (Alldrick, 1993; Smith, 1993; Barrett and Sherlock, 1996; Evenchick and McNicoll, 2002; MacDonald et al., 1996a; Macdonald et al., 1996b; Roth et al., 1999; Sherlock et al., 1999; Barresi and Dostal, 2005). Although upper Hazelton rocks appear to be developed along the Kitsault River valley hosting the Ag-rich Wolf deposit, preliminary mapping northwest and east of Kinskuch Lake suggests that only the lower part of the Hazelton Group is present, and rocks at the Dolly Varden deposit area appear to be similar to lower Hazelton Group rocks described in this study (intermediate tuff, lapilli tuff, porphyritic andesite; Devlin, 1987). The Kitsault River area also hosts porphyry Cu-Au systems (e.g., Big Bulk; Miller et al., 2020) and vein-hosted Au-Ag-Cu occurrences, which based on new geochronology data presented herein are likely related to magmatic activity during lower Hazelton Group volcanism.

The Dolly Varden and Wolf deposits contrast to the Eskay and Anyox deposits, both in mineralization type (e.g., Ag-rich versus Au- and Cu-rich), and host rock types (calc-alkaline intermediate-felsic volcanic rocks versus bimodal tholeiitic mafic to felsic volcanic rocks, some mudstone and mafic volcanic rocks). Similarities include complex stratiform and discordant vein-type mineralization styles with varying textures and mineralogy. The Eskay Creek deposit encompasses several stratiform to discordant Au-Ag-Pb-Zn-Cu zones with disseminated, massive to semi-massive sulphides and sulphosalts with varying amounts of barite content (Sherlock et al., 1999). The Anyox deposits consist of stratiform to stockwork Cu-Zn-Pb massive sulphide accumulations (MacDonald et al., 1996b) and the mineralization along the Dolly Varden trend are stratiform to slightly discordant Ag-Pb-Zn-barite deposits (Devlin and Godwin, 1986; Devlin, 1987). It seems that mineralization in the Kitsault River area was dispersed rather than focused in a discrete rift. Miller et al. (2020) present strong evidence for syndepositional faulting in the Kinskuch Lake area in the form of megaclast-bearing conglomerates similar to those described by Nelson and Kyba (2014) from the Jack Formation near the base of the Hazelton Group at Brucejack. We speculate that such syndepositional faults record extensional processes analogous to those that formed the Eskay rift and served as conduits for the passage of mineralizing hydro-magmatic fluids. Other Au-Ag-rich VMS-type mineralization in late Early to Middle Jurassic Hazelton Group rocks includes new discoveries southeast of the Brucejack Mine (Pretium Resources Inc., 2019), north of the Premier deposit at Silver Hill (Ascot Resources Ltd., 2019), and 30 km northeast of Stewart at Todd Creek (ArcWest Exploration Inc., 2019). These examples demonstrate the vast VMS-type mineralization potential of the Hazelton Group outside of the traditional Eskay rift.

8. Summary

Results from the first year of our multi-year study provide new resolution to the lower Hazelton Group stratigraphy and new U-Pb ages for the Hazelton Group and VMS-style mineralization in the Kitsault River area. The Hazelton Group rocks from Kitsault to Kinskuch Lake area are divided into three facies and two sub-facies. Facies 1 consists of lapilli tuff to tuff breccia with hornblende-plagioclase-phyric clasts and minor interbedded epiclastic rocks. Facies 2 consists mainly of epiclastic rocks. Facies 3 is predominantly lapilli tuff to tuff breccia with hornblende-plagioclase-phyric clasts and rare epiclastic rocks. Sub-facies 3a consists of K-feldspar-plagioclase porphyritic flows and lapilli tuff to tuff breccia with a plagioclase crystal-rich matrix and sub-facies 3b is a mixed unit with abundant volcanically derived tuff, lapilli tuff, and tuff breccia with thick limestone and mudstone-sandstone beds and local features indicating subaerial exposure. A sample of polymictic conglomerate from the base of the Hazelton Group yielded a maximum detrital zircon age (U-Pb, LA-ICPMS) of ca. 206 Ma, indicating that the onset of Hazelton Group volcanism was post-Rhaetian. A monzonite dike from the Homestake River deposit area returned a U-Pb CA-TIMS age of ca. 191 Ma suggesting the mineralization could be Early Jurassic. A lapilli tuff unit in the footwall of Ag-rich VMS mineralization at the Wolf deposit yielded a ca. 178 Ma age (U-Pb, LA-ICPMS), and a detrital zircon sample from a volcanic-derived sandstone yielded a maximum depositional age of ca. 169 Ma (U-Pb, LA-ICPMS), indicating that upper Hazelton Group units could be present in the Kitsault River valley close to the Dolly Varden mineralization trend.

Preliminary stratigraphic and geochronological results suggest that VMS-type mineralization in the Kitsault River area is related to shallow-level hydro-magmatic processes in an area of syndepositional faulting, parallel to the fully developed

Eskay rift. Coeval syngenetic mineralization systems in the two areas are likely related. Future work in the Kitsault River area will include geological mapping to better resolve the stratigraphy, timing, and geochemistry of the Hazelton Group.

Acknowledgments

We thank Dolly Varden Silver Corporation for logistical and helicopter support and a warm welcome in their Alice Arm exploration camp in 2015 and 2019. Cheerful and dedicated field assistance was provided by Meghan Holowath. Thanks to JoAnne Nelson for initiating reconnaissance studies in the Kitsault River area, co-collecting geochronology samples in 2015, and inspirational mentorship. A field visit in 2019 by Filippo Ferri was beneficial to our understanding of the field area. Chris Sebert is thanked for providing diamond drill hole geochronology samples, enlightening discussions, and showing us key outcrops and drill core in 2019. We also thank Richard Friedman (University of British Columbia, Vancouver) for providing preliminary U-Pb zircon geochronology results and Janet Gabites (University of British Columbia, Vancouver) for providing preliminary Ar-Ar K-feldspar geochronology results. A review by JoAnne Nelson significantly improved this manuscript.

References cited

Alldrick, D.J., 1993. Geology and metallogeny of the Stewart mining camp, northwestern British Columbia. British Columbia Ministry of Energy, Mines and Petroleum Resources, British Columbia Geological Survey Bulletin 85, 105 p.

Alldrick, D.J., Dawson, G.L., Bosher, J.A., and Webster, I.C.L., 1986. Geology of the Kitsault River area (NTS 103P). British Columbia Ministry of Energy, Mines and Petroleum Resources, British Columbia Geological Survey Open File 1986-02, 1:50,000 scale.

Anderson, R.G., 1989. A stratigraphic, plutonic and structural framework for the Iskut map area, northwestern British Columbia. In: Current Research, Part E, Geological Survey of Canada, Paper 89-1, pp. 145-154.

ArcWest Exploration Inc. 2019. ArcWest Exploration Inc. expands Yellow Bowl porphyry copper-gold target, Todd Creek project. https://arcwestexploration.com/2019/11/27/arcwest-exploration-inc-expands-yellow-bowl-porphyry-copper-gold-target-todd-creek-project/, last accessed December 2019.

Ascot Resources Ltd., 2019. Ascot intersects 880 g/t silver over 1.00 metre at new Silver Hill target. https://ascotgold.com/news-releases/2019/ascot-intersects-880g-t-silver-over-1.00-metre-at-new-silver-hill-target/, last accessed December 2019.

Barresi, T., and Dostal, J., 2005. Geochemistry and petrography of upper Hazelton Group volcanics: VHMS-favourable stratigraphy in the Iskut River and Telegraph Creek map areas, northwestern British Columbia. In: Geological Fieldwork 2004, British Columbia Ministry of Energy and Mines, British Columbia Geological Survey Paper 2005-1, pp. 39-47.

Barresi, T., Nelson, J.L., and Dostal, J., 2015. Geochemical constraints on magmatic and metallogenic processes: Iskut River Formation, volcanogenic massive sulfide-hosting basalts, NW British Columbia, Canada. Canadian Journal of Earth Sciences, 52, 1-20.

Barrett, T.J., and Sherlock, R.L., 1996. Geology, lithogeochemistry and volcanic setting of the Eskay Creek Au-Ag-Cu-Zn deposit, northwestern British Columbia. Exploration and Mining Geology, 5, 339-368.

Black, J.M., 1951. Geology and mineral occurrences of the Upper Kitsault Valley. In: British Columbia Ministry of Energy, Mines and Petroleum Resources, British Columbia Geological Survey Annual Report, pp. A76-A83.

Brown, D.A., Gunning, M.H., and Greig, C.J., 1996. The Stikine project: Geology of western Telegraph Creek map area, northwestern British Columbia. British Columbia Ministry of Employment and Investment, British Columbia Geological Survey Bulletin 95, 130 p.

Campbell, F.A., 1959. The geology of Torbrit Silver Mine, British Columbia. Economic Geology, 54, 1461-1495. doi: 10.2113/gsecongeo.54.8.1461.

Carter, N.C., 1981. Porphyry copper and molybdenum deposits, west-central British Columbia. In: British Columbia Ministry of Energy Mines and Petroleum Resources, British Columbia Geological Survey Bulletin 64, 81 p.

Childe, F., 1996. U-Pb geochronology and Nd and Pb isotope characteristics of the Au-Ag-rich Eskay Creek volcanogenic massive sulfide deposit, British Columbia. Economic Geology, 91, 1209-1224. doi: 10.2113/gsecongeo.91.7.1209.

Childe, F.C., 1997. Timing and tectonic setting of volcanogenic massive sulphide deposits in British Columbia: constraints from U-Pb geochronology, radiogenic isotopes, and geochemistry. Unpublished Ph.D. thesis, The University of British Columbia, Vancouver, B.C., Canada. Available from https://circle.ubc.ca/handle/2429/7311 accessed April, 2012.

Colpron, M., Nelson, J.L., and Murphy, D.C., 2007. Northern Cordilleran terranes and their interactions through time. GSA Today, 17, 4-10.

Coney, P.J., Jones, D.L., and Monger, J.W.H., 1980. Cordilleran suspect terranes. Nature, 288, 329-333. doi: 10.1038/288329a0.

Coutts, D.S., Matthews, W.A., and Hubbard, S.M., 2019. Assessment of widely used methods to derive depositional ages from detrital zircon populations. Geoscience Frontiers, 10, 1421-1435. doi: 10.1016/j.gsf.2018.11.002.

Dawson, G.L., and Alldrick, D.J., 1986. Geology and mineral deposits of the Kitsault Valley. In: Geological Fieldwork 1985, British Columbia Ministry of Energy, Mines and Petroleum Resources, British Columbia Geological Survey Paper 1986-1, pp. 219-224.

Devlin, B.D., 1987. Geology and genesis of the Dolly Varden silver camp, Alice Arm area, northwestern British Columbia. Unpublished M.Sc. thesis, The University of British Columbia, Vancouver, B.C., Canada. Available from https://open.library.ubc.ca/cIRcle/collections/ubctheses/831/items/1.0052815 accessed November 5, 2015.

Devlin, B.D., and Godwin, C.I., 1986. Geology of the Dolly Varden camp, Alice Arm area. In: Geological Fieldwork 1985, British Columbia Ministry of Energy, Mines and Petroleum Resources, British Columbia Geological Survey Paper 1986-1, pp. 327-330.

Diakow, L.J., Panteleyev, A., and Schroeter, T.G., 1991. Jurassic epithermal deposits in the Toodoggone River area, northern British Columbia; examples of well-preserved, volcanic-hosted, precious metal mineralization. Economic Geology, 86, 529-554. doi: 10.2113/gsecongeo.86.3.529.

Dickinson, W.R., and Gehrels, G.E., 2009. Use of U-Pb ages of detrital zircons to infer maximum depositional ages of strata: A test against a Colorado Plateau Mesozoic database. Earth and Planetary Science Letters, 288, 115-125. doi: 10.1016/j.epsl.2009.09.013.

Dott, R.H., 1964. Wacke, graywacke and matrix; what approach to immature sandstone classification? Journal of Sedimentary Research, 34, 625-632. doi: 10.1306/74D71109-2B21-11D7-8648000102C1865D.

Dunne, K.P.E., and Pinsent, R.H., 2002. Depositional setting of silver-rich quartz-sulphate-carbonate deposits of the upper Kitsault River area, northwest British Columbia. In: Geological Fieldwork 2001, British Columbia Ministry of Energy, Mines and Petroleum

Resources, British Columbia Geological Survey Paper 2002-01, pp. 177-196.
Eisbacher, G.H., 1981. Late Mesozoic-Paleogene Bowser Basin molasse and Cordilleran tectonics, western Canada. In: Miall, A.D., (Ed.), Sedimentation and Tectonics in Alluvial Basins, Geological Association of Canada Special Paper 23, pp. 125-151.
Evenchick, C.A., and McNicoll, V.J., 2002. Stratigraphy, structure, and geochronology of the Anyox Pendant, northwest British Columbia, and implications for mineral exploration. Canadian Journal of Earth Sciences, 39, 1313-1332. doi: 10.1139/e02-036.
Evenchick, C.A., and Thorkelson, D.J., 2005. Geology of the Spatsizi River map area, north-central British Columbia. Geological Survey of Canada Bulletin 577, 276 p.
Evenchick, C.A., McMechan, M.E., McNicoll, V.J., and Carr, S.D., 2007. A synthesis of the Jurassic-Cretaceous tectonic evolution of the central and southeastern Canadian Cordillera: Exploring links across the orogen. In: Sears, J.W., Harms, T.A. and Evenchick, C.A., (Eds.), Whence the mountains? Inquiries in the evolution of orogenic systems: A volume in honor or Raymond A. Price, Geological Society of America Special Paper 433, pp. 117-145.
Evenchick, C.A., Mustard, P.S., Greig, C.J., McMechan, M.E., Ritcey, D.H., Smith, G.T., and Ferri, F., 2008. Geology, Nass River, British Columbia. Open File, Geological Survey of Canada. Available from http://geoscan.ess.nrcan.gc.ca/cgi-bin/starfinder/0?path=geoscan.fl&id=fastlink&pass=&search=R%3D225792&format=FLFULL accessed June 9, 2015.
Fisher, R.V., 1966. Rocks composed of volcanic fragments. Earth-Science Reviews, 1, 287-298.
Franklin, J.M., Gibson, H.L., Jonasson, I.R., and Galley, A.G., 2005. Volcanogenic massive sulfide deposits. In: Hedenquist, J.W., Thompson, J.F.H., Goldfarb, R.J., and Richards, J.P., (Eds.), Economic Geology 100th Anniversary Volume, The Economic Geology Publishing Company, pp. 523-560.
Gagnon, J.-F., Barresi, T., Waldron, J.W.F., Nelson, J.L., Poulton, T.P., and Cordey, F., 2012. Stratigraphy of the upper Hazelton Group and the Jurassic evolution of the Stikine terrane, British Columbia. Canadian Journal of Earth Sciences, 49, 1027-1052. doi: 10.1139/e2012-042.
Galley, A.G., Hannington, M.D., and Jonasson, M., 2007. Volcanogenic massive sulphide deposits. In: Goodfellow, W.D., (Ed.), Mineral deposits of Canada: A synthesis of major deposit types, district metallogeny, the evolution of geological provinces, and exploration methods, Geological Association of Canada, Mineral Deposits Division, Special Publication 5, pp. 141-161.
Godwin, C.I., Pickering, D.R., Gabites, J.E., and Alldrick, D.J., 1991. Interpretation of galena lead isotopes from the Stewart-Iskut area (103O, P; 104A, B G). In: Geological Fieldwork 1990, British Columbia Ministry of Energy and Mines, British Columbia Geological Survey Paper 1991-01, pp. 235-243.
Greig, C.J., 1991. Stratigraphic and structural relations along the west-central margin of the Bowser Basin, Oweegee and Kinskuch areas, northwestern British Columbia. In: Current Research, Part A, Geological Survey of Canada Paper 91-1A, pp. 197-205.
Greig, C.J., 1992. Jurassic and Cretaceous plutonic and structural styles of the Eagle Plutonic Complex, southwestern British Columbia, and their regional significance. Canadian Journal of Earth Sciences, 29, 793-811. doi: 10.1139/e92-067.
Greig, C., 2014. Latest Triassic-Earliest Jurassic contractional deformation, uplift and erosion in Stikinia, northwest British Columbia. 2014 GSA Annual Meeting in Vancouver, British Columbia (19-22 October 2014), GSA. Available from https://gsa.confex.com/gsa/2014AM/webprogram/Paper248914.html accessed November 8, 2019.
Greig, C.J., and Gehrels, G.E., 1995. U-Pb zircon geochronology of Lower Jurassic and Paleozoic Stikinian strata and Tertiary intrusions, northwestern British Columbia. Canadian Journal of Earth Sciences, 32, 1155-1171. doi: 10.1139/e95-095.
Greig, C.J., Anderson, R.G., Daubeny, P.H., and Bull, K.F., 1994. Geology of the Cambria Icefield: Stewart (103P/13), Bear River (104A/4), and parts of Meziadin Lake (104A/3) and Paw Lake (103P/12) map areas, northwestern British Columbia, 1:50,000 scale.
Grove, E.W., 1986. Geology and mineral deposits of the Stewart area, British Columbia. British Columbia Ministry of Energy, Mines and Petroleum Resources, British Columbia Geological Survey Bulletin 58, 219 p.
Hanson, G., 1922. Upper Kitsault Valley, British Columbia. In: Geological Survey of Canada, Summary Report Part A, pp. 7-21.
Hanson, G., 1923. Reconnaissance between the Skeena River and Stewart, British Columbia. In: Geological Survey of Canada, Summary Report Part A, pp. 29-45.
Hanson, G., 1928. Mineral deposits of the Alice Arm district. In: Geological Survey of Canada, Summary Report Part A, p. 27.
Henry, C.D., Elson, H.B., McIntosh, W.C., Heizler, M.T., and Castor, S.B., 1997. Brief duration of hydrothermal activity at Round Mountain, Nevada, determined from $^{40}Ar/^{39}Ar$ geochronology. Economic Geology, 92, 807-826. doi: 10.2113/gsecongeo.92.7-8.807.
Herriott, T.M., Crowley, J.L., Schmitz, M.D., Wartes, M.A., and Gillis, R.J., 2019. Exploring the law of detrital zircon: LA-ICP-MS and CA-TIMS geochronology of Jurassic forearc strata, Cook Inlet, Alaska, USA. Geology, 47, 1044-1048. doi: 10.1130/G46312.1.
Higgs, A.A., 2015. 2015 Technical Report for the Dolly Varden Property, Skeena Mining Division (NTS 103P/11, 12, 13, and 14), 133p, https://www.dollyvardensilver.com/site/assets/files/1326/dv-2015-04-16-43-101-technical-report.pdf, last accessed December 2019.
Hoy, T., 1991. Volcanogenic massive sulphide deposits in British Columbia. In: McMillan, W.J., (Ed.), Ore Deposits, Tectonics and Metallogeny in the Canadian Cordillera, British Columbia Ministry of Energy, Mines and Petroleum Resources, British Columbia Geological Survey Paper 1991-4, pp. 89-124.
Kelley, S., 2002. K-Ar and Ar-Ar dating. Reviews in Mineralogy and Geochemistry, 47, 785-818. doi: 10.2138/rmg.2002.47.17.
Large, R.R., McPhie, J., Gemmell, J.B., Herrmann, W., and Davidson, G.J., 2001. The spectrum of ore deposit types, volcanic environments, alteration halos, and related exploration vectors in submarine volcanic successions: Some examples from Australia. Economic Geology, 96, 913-938. doi: 10.2113/gsecongeo.96.5.913.
Logan, J.M., Drobe, J.R., and McClelland, W.C., 2000. Geology of the Forrest Kerr-Mess Creek area, northwestern British Columbia. British Columbia Geological Survey Bulletin 104, 132 p.
Logan, J.M., and Mihalynuk, M.G., 2014. Tectonic controls on Early Mesozoic paired alkaline porphyry deposit belts (Cu-Au ±Ag-Pt-Pd-Mo) within the Canadian Cordillera. Economic Geology, 109, 827-858. doi: 10.2113/econgeo.109.4.827.
Ludwig, K.R., 2012. Isoplot 3.75. A geochronological toolkit for Microsoft Excel. Special Publication, Berkley Geochronology Center, 75 p.
MacDonald, A.J., 1993. Lithostratigraphy and geochronometry, Brucejack Lake, northwestern British Columbia (104B/08E). In: Geological Fieldwork 1992, British Columbia Ministry of Energy and Mines, British Columbia Geological Survey Paper 1993-1, pp. 315-323.
Macdonald, A.J., Lewis, P.D., Thompson, J.F.H., Nadaraju, G., Bartsch, R., Bridge, D.J., Rhys, D.A., Roth, T., Kaip, A., Godwin, C.I., and Sinclair, A.J., 1996a. Metallogeny of an Early to Middle Jurassic arc, Iskut River area, northwestern British Columbia. Economic Geology, 91, 1098-1114. doi: 10.2113/gsecongeo.91.6.1098.
MacDonald, R.W.J., Barrett, T.J., and Sherlock, R.L., 1996b. Geology and lithogeochemistry at the Hidden Creek massive

sulfide deposit, Anyox, west-central British Columbia. Exploration and Mining Geology, 5, 369-398.

MacIntyre, D., Ash, C., and Britton, J., 1994. Geological compilation Skeena-Nass area, west central British Columbia. In: British Columbia Ministry of Energy, Mines and Petroleum Resources, British Columbia Geological Survey Open File 1994-14, 1:250,000 scale.

Marsden, H., and Thorkelson, D.J., 1992. Geology of the Hazelton volcanic belt in British Columbia: Implications for the Early to Middle Jurassic evolution of Stikinia. Tectonics, 11, pp. 1266-1287. doi: 199210.1029/92TC00276.

McConnell, R.G., 1913. Portions of Portland Canal and Skeena Mining Divisions, Skeena District, British Columbia. Geological Survey of Canada, Memoir 32, 101 p.

McCuaig, M., and Sebert, C., 2017. 2016 Technical Report for the Dolly Varden Property, Skeena Mining Division. British Columbia Ministry of Energy, Mines and Petroleum Resources Assessment Report 36934.

McPhie, J., Doyle, M., and Allen, R., 1993. Volcanic textures. A guide to the interpretation of textures in volcanic rocks. Centre for Ore Deposits and Exploration Studies, University of Tasmania, Hobart, Australia, 198 p.

Miller, E.A., Kennedy, L.A., and van Straaten, B.I., 2020. Geology of the Kinskuch Lake area and Big Bulk porphyry prospect: Syndepositional faulting and local basin formation during the Rhaetian (latest Triassic) transition from the Stuhini to the Hazelton Group In: Geological Fieldwork 2019, British Columbia Ministry of Energy, Mines and Petroleum Resources, British Columbia Geological Survey Paper 2020-01, pp. 77-99.

Monger, J.W.H., 1977. The Triassic Takla Group in McConnell Creek map-area, north central British Columbia. Geological Survey of Canada Paper 76-29, 45 p.

Monger, J.W.H., Price, R.A., and Tempelman-Kluit, D.J., 1982. Tectonic accretion and the origin of the two major metamorphic and plutonic welts in the Canadian Cordillera. Geology, 10, 70-75. doi: 10.1130/0091-7613(1982)10<70:TAATOO>2.0.CO;2.

Monger, J.W.H., Wheeler, J.O., Tipper, H.W., Gabrielse, H., Harms, T., Struik, L.C., Campbell, R.B., Dodds, C.J., Gehrels, G.E., and O'Brien, J., 1991. Part B. Cordilleran Terranes. In: Gabrielse, H., and Yorath, C.J., (Eds.), Upper Devonian to Middle Jurassic assemblages, Chapter 8, Geology of the Cordilleran Orogen in Canada 4, pp. 281-327.

Mortensen, J.K., and Kirkham, R.V., 1992. A U-Pb zircon age for host rocks of a syngenetic strontium(-zinc) occurrence in the Kitsault Lake area, west-central British Columbia. In: Radiogenic Age and Isotopic Studies, Report 5, Geological Survey of Canada, Paper 91.2, pp. 181-185.

Nelson, J.L., Colpron, M., and Israel, S., 2013. The Cordillera of British Columbia, Yukon and Alaska: Tectonics and metallogeny. In: Colpron, M., Bissig, T., Rusk, B. G., and Thompson, J., (Eds.), Tectonics, Metallogeny and Discovery: The North American Cordillera and Similar Accretionary Settings, Society of Economic Geologists Special Publication 17, pp. 53-110.

Nelson, J.L., and Kyba, J., 2014. Structural and stratigraphic control of porphyry and related mineralization in the Treaty Glacier-KSM-Brucejack-Stewart trend of western Stikinia. In: Geological Fieldwork 2013, British Columbia Ministry of Energy, Mines and Petroleum Resources, British Columbia Geological Survey Paper 2014-1, pp. 111-140.

Nelson, J.L., Waldron, J., van Straaten, B.I., Zagorevski, A., and Rees, C., 2018. Revised stratigraphy of the Hazelton Group in the Iskut River region, northwestern British Columbia. In: Geological Fieldwork 2017, British Columbia Ministry of Energy, Mines and Petroleum Resources, British Columbia Geological Survey Paper 2018-1, pp. 15-38.

Orton, G.J., 1995. Facies models in volcanic terrains: Time's arrow versus time's cycle. In: Plint, A.G., (Ed.), Sedimentary Facies Analysis, International Association of Sedimentologists Special Publication 22, pp. 157-193.

Pinsent, R.H., 2001. Mineral deposits of the upper Kitsault River area, British Columbia. In: Geological Fieldwork 2000, British Columbia Ministry of Energy and Mines, British Columbia Geological Survey Paper 2001-1, pp. 313-326.

Pretium Resources Inc., 2019. Pretium exploration and Brucejack update. https://www.pretivm.com/news/news-release-details/2019/Pretivm-Exploration-And-Brucejack-Update/default.aspx, last accessed December 2019.

Ross, D., and Chamois, P., 2017. Technical report on the Homestake Ridge project, Skeena mining division, northwestern British Columbia. Report prepared for Auryn Resources Inc., https://www.aurynresources.com/site/assets/files/2343/auryn_resources_homestake_ridge_ni_43-101_23oct2017.pdf, last accessed December 2019.

Roth, T., Thompson, J.F.H., and Barrett, T.J., 1999. The precious metal-rich Eskay Creek deposit, northwestern British Columbia. In: Barrie, C. T., and Hannington, M.D., (Eds.), Volcanic-associated massive sulfide deposits: processes and examples in modern and ancient setting, Reviews in Economic Geology 8, pp. 357-374.

Schmid, R., 1981. Descriptive nomenclature and classification of pyroclastic deposits and fragments: Recommendations of the IUGS Subcommission on the Systematics of Igneous Rocks. Geology, 9, 41-43. doi: 10.1130/0091-7613(1981)9<41:DNACOP>2.0.CO;2.

Sebert, C., and Ramsay, A., 2012. Technical report on the Wolf deposit 2011 exploration program: Geology and diamond drilling. Ministry of Energy and Mines, British Columbia Geological Survey Assessment Report 33326, 55 p.

Sherlock, R.L., Roth, T., Spooner, E.T.C., and Bray, C.J., 1999. Origin of the Eskay Creek precious metal-rich volcanogenic massive sulfide deposit; fluid inclusion and stable isotope evidence. Economic Geology, 94, 803-824. doi: 10.2113/gsecongeo.94.6.803.

Smith, A.D., 1993. Geochemistry and tectonic setting of volcanics from the Anyox mining camp, British Columbia. Canadian Journal of Earth Sciences, 30, 48-59. doi: 10.1139/e93-005.

Streepey, M.M., Hall, C.M., and van der Pluijm, B.A., 2002. The ^{40}Ar-^{39}Ar laser analysis of K-feldspar: Constraints on the uplift history of the Grenville Province in Ontario and New York. Journal of Geophysical Research: Solid Earth, 107, 1-11. doi: 10.1029/2001JB001094.

Swanton, D., Baker, D., Hughes, C., Marsden, H., and Lajoie, J., 2013. 2013 diamond drilling, geological, geochemical and geophysical report Homestake Ridge project. Ministry of Energy and Mines, British Columbia Geological Survey Assessment Report 34433, 94 p.

Tipper, H.W., and Richards, T.A., 1976. Jurassic stratigraphy and history of north-central British Columbia. Geological Survey of Canada Bulletin 270, 82 p.

Turnbull, J.M., 1916. Alice Arm district. In: British Columbia Ministry of Energy Mines and Petroleum Resources, British Columbia Geological Survey Annual Report 1916, pp. 53-84.

Turner, A.J., and Nicholls, S.J., 2019. Technical report and mineral resource update for the Dolly Varden property, British Columbia, Canada. NI 43-101 Report prepared for Dolly Varden Silver Corporation, 175p, https://www.dollyvardensilver.com/site/assets/files/1652/dolly-varden-ni43-101-21june2019-apex.pdf, last accessed December 2019.

Wheeler, J.O., Brookfield, A.J., Gabrielse, H., Monger, J.W.H., Tipper, H.W., and Woodsworth, G.J., 1991. Terrane map of the Canadian Cordillera. Geological Survey of Canada Map 1713A, 1:2,000,000 scale.